Dalton Transactions

RSC Publishing

PAPER

View Article Online
View Journal | View Issue

Cite this: *Dalton Trans.*, 2013, **42**, 3373

Selective borane reduction of phosphinoferrocene carbaldehydes to phosphinoalcohol–borane adducts. The coordination behaviour of 1-(diphenylphosphino)-1′-(methoxymethyl)ferrocene, a new ferrocene O,P-hybrid donor prepared from such an adduct†

Petr Štěpnička* and Ivana Císařová

The reduction of ferrocene phosphino-aldehydes, R_2PfcCHO (R = Ph, **2**; Cy, **3**; fc = ferrocene-1,1′-diyl, Cy = cyclohexyl) and (S_p)-[Fe(η^5-C_5H_3-1-CHO-2-PPh_2)(η^5-C_5H_5)] ((S_p)-**4**), with BH_3·THF or BH_3·SMe_2 in THF at 0 °C selectively afforded the corresponding phosphinoalcohol–borane adducts, R_2PfcCH_2OH·BH_3 (R = Ph, **5**; Cy, **6**) and (S_p)-[Fe(η^5-C_5H_3-1-CH_2OH-2-PPh_2)(η^5-C_5H_5)]·BH_3 ((S_p)-**7**), in quantitative yields. In contrast, the reactions performed at elevated temperatures favoured the formation of methyl derivatives (*e.g.*, Ph_2PfcCH_3·BH_3 (**8**)) resulting from overreduction (deoxygenation). The crystal structures of **3**, **5**, (S_p)-**7**, **8** and Cy_2PfcBr (**9**) have been determined by single-crystal X-ray diffraction analysis. The crystal assemblies of adducts **5** and (S_p)-**7** are built up by means of C–H···O contacts, O–H···HB dihydrogen bonds and other soft interactions but, surprisingly, not *via* the conventional O–H···O hydrogen bonds. Adduct **5** was smoothly deprotected to give the corresponding free phosphine, Ph_2PfcCH_2OH (**1**), and was further used for the preparation of a hybrid phosphinoether ligand, Ph_2PfcCH_2OMe (**11**). The latter compound was studied as a donor for Group 8–10 metal ions and for Cu(I), whereupon the following complexes were isolated and structurally characterised: [(η^6-*p*-cymene)$RuCl_2$(**11**-κ*P*)] (**12***), [(η^6-*p*-cymene)RuCl(**11**-κ*P*)(MeCN)][SbF_6] (**13***), [RhCl(cod)(**11**-κ*P*)] (cod = η^2:η^2-cycloocta-1,5-diene; **14**), *trans*-[$PdCl_2$(**11**-κ*P*)$_2$] (*trans*-**15***), [PdCl(μ-Cl)(**11**-κ*P*)]$_2$ (**16***), *cis*- and *trans*-[$PtCl_2$(**11**-κ*P*)$_2$] (*cis*-**17** and *trans*-**17***), and [Cu(CF_3SO_3-κ*O*)(**11**-κ*P*)(H_2O)] (**18**) (the asterisk indicates that the crystal structure was determined). In all these compounds, ligand **11** behaves as a P-monodentate donor while its ether group remains uncoordinated. This probably reflects structural flexibility of **11** resulting from the presence of the methylene linker and also distinguishes **11** from its known, non-spaced analogue Ph_2PfcOMe.

Received 21st October 2012,
Accepted 27th November 2012

DOI: 10.1039/c2dt32511j

www.rsc.org/dalton

Introduction

Investigations into phosphinoferrocene ligands started rather unobtrusively with the syntheses of (diphenylphosphino)ferrocene[1] and 1,1′-bis(diphenylphosphino)ferrocene (dppf)[2] in the mid-1960s. These studies continue with unremitting vigour and have resulted in a vast family of structurally versatile ligands, among which dppf and related compounds still play an important role.[3,4]

Numerous practical applications of dppf in coordination chemistry and catalysis obviously prompted the preparation of its congeners. Several approaches towards the modification of the parent dppf molecule are now established in the literature, one particular method being the replacement of one phosphine group with another functional moiety (FG in Scheme 1).

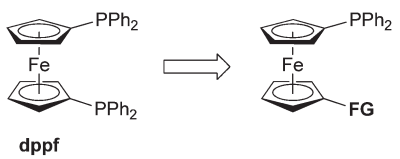

Scheme 1 One of possible approaches towards modifications of the parent dppf structure (**FG** denotes a functional substituent).

Department of Inorganic Chemistry, Faculty of Science, Charles University in Prague, Hlavova 2030, 12840 Prague 2, Czech Republic. E-mail: stepnic@natur.cuni.cz; Fax: +420 221 951 253

†Electronic supplementary information (ESI) available: The synthesis and crystal structures of **3** and **9**, description of the crystal packing of **5**, view of the crystal structure of *trans*-**17**, a view of the coordination sphere and the crystal packing diagram for **18**, and a summary of the crystallographic data in a tabular form. CCDC 906406–906418. For ESI and crystallographic data in CIF or other electronic format see DOI: 10.1039/c2dt32511j

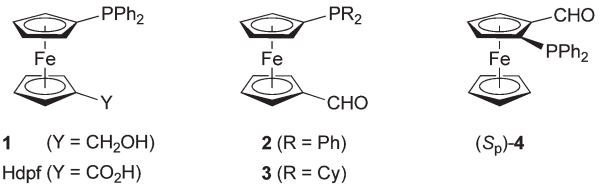

1 (Y = CH_2OH) Hdpf (Y = CO_2H) **2** (R = Ph) **3** (R = Cy) (S_p)-**4**

Scheme 2 Structural drawings of alcohol **1**, Hdpf and aldehydes used in this study (Cy = cyclohexyl).

The application of this approach resulted in a number of interesting donor-asymmetric ligands of the type Ph_2PfcY,[5] where fc is ferrocene-1,1′-diyl and Y is a (non-phosphine) donor group or a functional moiety.[5,6]

In the search for alternative phosphinoferrocene synthetic building blocks, we prepared [1′-(diphenylphosphino)ferrocen-1-yl]methanol (**1**, Scheme 2)[7] *via* hydride reduction of 1′-(diphenylphosphino)ferrocene-1-carbaldehyde (**2**)[7,8] and the corresponding carboxylic acid (Hdpf).[9–11] This alcohol was recently shown to be a good starting material for the preparation of a semi-homologous dppf congener, $Ph_2PfcCH_2PPh_2$,[6i] which led us to search for similar building blocks and their synthetic applications, mainly in the preparation of phosphinoferrocene ligands. It is notable that similar phosphino–alcohol synthons have been used only scarcely in ferrocene chemistry[12] and had to be protected during some parts of the reaction sequence owing to the presence of the oxidation-sensitive phosphine moiety.[13]

With an aim of further developing the synthetic applications of phosphinoferrocene alcohols, we decided to study the reduction of phosphinoferrocene carbaldehydes with borane as a classical though 'non-innocent' reducing agent,[14] which itself can serve as a phosphine protecting group.[15] In this contribution, we describe our study on borane reduction of the representative phosphinoferrocene aldehydes **2**, **3** and (S_p)-**4** (Scheme 2) and a detailed characterisation of the resulting phosphinoalcohol–borane adducts. Furthermore, we demonstrate the synthetic potential of these adducts by a two-step conversion of [1′-(diphenylphosphino)ferrocene-1-yl]-methanol–borane (1/1) (*i.e.*, **1**·BH_3) as a representative to 1′-(diphenylphosphino)-1-(methoxymethyl)ferrocene and report our investigations into the coordination behaviour of this novel O,P-hybrid[16] ferrocene ligand towards Group 8–10 metal cations and copper(I).

Results and discussion

Borane reduction of phosphinoferrocene aldehydes

The reduction of ferrocenecarbonyl compounds FcC(O)R, where Fc is ferrocenyl and R is H or an organyl group, with various hydridoboron agents (*e.g.*, BH_3·SMe_2,[17,18] $NaBH_4$–CF_3CO_2H,[19] BF_3·OEt_2–$NaBH_3(CN)$,[20] $TiCl_4$–$NaBH_3(CN)$,[21] Zn-$(BH_4)_2$–$ZnCl_2$ [22]) was previously demonstrated to proceed in an exhaustive manner to afford the respective alkylferrocenes, $FcCH_2R$. Borane-dimethylsulphide was further shown to

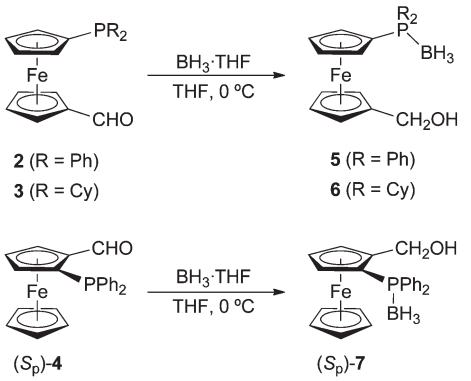

2 (R = Ph) **3** (R = Cy) **5** (R = Ph) **6** (R = Cy)

(S_p)-**4** (S_p)-**7**

Scheme 3 Borane-reduction of phosphinoaldehydes **2**, **3** and (S_p)-**4**.

similarly deoxygenate ferrocenecarboxylic acid and the related alcohols FcCH(OH)R.[17] An analogous reaction was reported even for phosphine-aldehyde (S_p)-**4**, which was converted to (S_p)-2-(diphenylphosphino)-1-methylferrocene–borane (1/1) upon reacting with BH_3·SMe_2 (3 equiv.) at room temperature for 16 h.[18]

We found that when the reduction is performed with the simple aldehyde **2** and an excess of borane dissolved in THF (*i.e.*, with commercially available BH_3·THF in THF) at 0 °C, it takes a different course, affording rapidly and selectively phosphinoalcohol–borane adduct **5** (Scheme 3). Adduct $FcPPh_2$·BH_3, detected as the only minor side product in the crude reaction mixture,[23] resulted from the direct borylation of (diphenylphosphino)ferrocene, which is notoriously present in **2** as a trace impurity.[24] This compound was efficiently removed by column chromatography on silica gel, which then furnished analytically pure **5** in practically quantitative yield.

The selective formation of **5**, a product type different from what was previously detected, led us to elucidate a possible influence of the reaction conditions on the reaction course. When the reaction mixture was heated at reflux in THF overnight, it afforded a mixture of alcohol **5** and 1-(diphenylphosphino)-1′-methylferrocene–borane (**8**), resulting from exhaustive reduction. The latter, deoxygenated compound was isolated in quantitative yield upon replacing BH_3·THF with BH_3·SMe_2 (1 M in THF; refluxing in THF overnight), which is indeed in line with the previous observations.[18] The difference in the reactivity of BH_3·THF and BH_3·SMe_2 (*i.e.*, partial *vs.* exhaustive reduction) can be accounted for by the greater thermal stability of the latter borane adduct. This assumption, based on empirical observations,[25] is supported by theoretical computations, showing that the hypothetical reaction of BH_3 with H_2S to form an adduct is more exothermic than that with H_2O.[26]

In order to verify whether the discovered selective partial reduction represents a generally applicable transformation, similar reactions were carried out with aldehyde **3** bearing a different phosphino group and with the isomeric, planar-chiral aldehyde (S_p)-**4**.[11b] Aldehyde **3** was prepared analogously to **2**[7] from 1,1′-dibromoferrocene (Scheme 4). The dibromide was first converted[27] to phosphine-bromide **9** by lithiation and

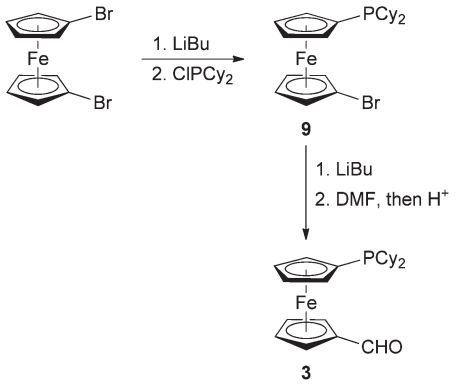

Scheme 4 Preparation of aldehyde **3** (DMF = *N*,*N*-dimethylformamide).

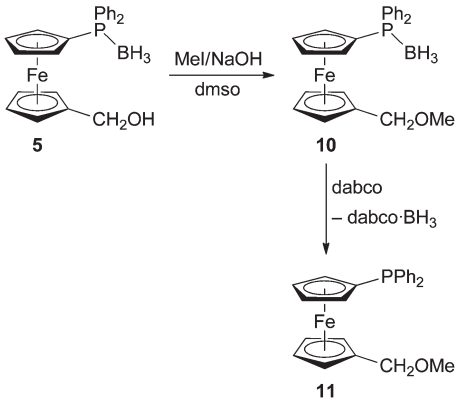

Scheme 5 Preparation of phosphine-ether **11** (dabco = 1,4-diazabicyclo-[2.2.2]octane).

reaction with $ClPCy_2$. In a similar manner, intermediate **9** was lithiated and carbonylated with *N*,*N*-dimethylformamide to give aldehyde **3**. Compounds **3** and **9** were fully characterised by spectroscopic methods and their molecular structures were determined by X-ray diffraction analysis (see ESI†).

The reduction of **3** with BH_3–THF proceeded similarly to **2**, producing the corresponding adduct **6** (Scheme 3; 97% isolated yield). Likewise, the borane reduction of (S_p)-**4** cleanly produced adduct (S_p)-**7** (Scheme 3) as a viscous oil. According to the analytical data, the product isolated by simple flash column chromatography was essentially pure. Any further 'purification' of (S_p)-**7** proved rather difficult due to a tendency to retain traces of the solvents and a reluctance to crystallise. Nonetheless, crystals of (S_p)-**7** suitable for X-ray diffraction analysis were obtained by crystallisation from hot heptane (*vide infra*).

The reduction of phosphinoferrocene aldehydes **2**, **3** and (S_p)-**4** was clearly manifested in the ^1H and ^{13}C NMR spectra by a disappearance of the characteristic resonances due to the formyl substituents, which were replaced by the signals of the hydroxymethyl groups. The resulting adducts displayed typical broad signals of the BH_3 protons in their ^1H NMR spectra and broad doublet-like resonances in the ^{31}P NMR spectra. Besides, the progress of the reduction reaction was nicely indicated by a colour change from the initial red-orange to orange-yellow reflecting a loss of conjugation.

Preparation of phosphinoether ligand 11

Aiming at synthetic utilisation of the obtained phosphinoalcohol–borane adducts, we first studied the possibility of deprotecting the phosphine moiety. Gratifyingly, the BH_3 group was smoothly removed upon reacting the representative adduct **5** with 1,4-diazabicyclo[2.2.2]octane (dabco) in C_6D_6 (60 °C/3 h) to afford alcohol **1**.[15] This encouraged us to use adduct **5** further in the preparation of new phosphinoferrocene ligands.

Thus, a mixed-donor phosphinoether ligand **11** was synthesised (Scheme 5) by alkylation of alcohol **5** with NaOH–CH_3I in dry dimethylsulphoxide, affording intermediate adduct **10**, and by the subsequent removal of the protecting BH_3 group with dabco. This procedure provided **11** as an orange-yellow solid in an 85% yield.

Compounds **10** and **11** were characterised by the usual spectroscopic methods and their crystal structures have been determined by X-ray diffraction analysis. Successful methylation of **5** was manifested by the signals of the methoxymethyl group (**10**: CH_2, δ_H 3.88, δ_C 69.88; OMe, δ_H 3.22, δ_C 57.79; **11**: CH_2, δ_H 3.96, δ_C 70.31; OMe, δ_H 3.24, δ_C 57.68), whereas deborylation was clearly demonstrated in the ^{31}P NMR spectra (*cf.* δ_P: 16.4 for **10**, and −16.3 for **11**).

The crystal structures of 5, (S_p)-7, 8, 10 and 11

The molecular structures of **5**, **8** and (S_p)-**7** are depicted in Fig. 1–3. Compounds **5** and **8** are virtually isostructural, crystallising with the symmetry of the monoclinic space group $P2_1/c$ and *four* structurally independent molecules (for geometric data, see Tables 1 and 2). Compound (S_p)-**7** crystallises in the orthorhombic space group $P2_12_12_1$ and one molecule per asymmetric unit.

Structural parameters determined for **8**, **5** and (S_p)-**7** lie within the common ranges and compare well with the data reported for $FcCH_2OH$,[28] **1**,[7] [2-(diphenylphosphino)ferrocen-1-yl]methanol,[29] and various phosphinoferrocene–BH_3 adducts.[18,30] The ferrocene units in the independent molecules of **5** exert similar Fe-ring centroid (Cg) distances and negligible tilting (Table 1) while their substituents assume conformations close to synclinal eclipsed as indicated by the torsion angles C*n*01–Cg(P,*n*)–Cg(C,*n*)–C*n*06 of 77–78° (*n* = 1–4; *cf.* the theoretical value 72°).

Similarly, the parameters determined for the structurally independent albeit practically undistinguishable molecules of **8** (Table 2) do not depart from the values reported for 1,1′-dimethylferrocene[31] and the BH_3 adducts mentioned above.[18,30] The ferrocene moieties are regular showing tilt angles below 2° and synclinal eclipsed conformations with τ = 79–80°. The fact that the Fe–Cg(P) distances are slightly but statistically significantly shorter (0.010–0.016 Å) than their matched Fe–Cp(C) distances in all the four molecules probably reflects strengthening of the Fe–C bonds upon the

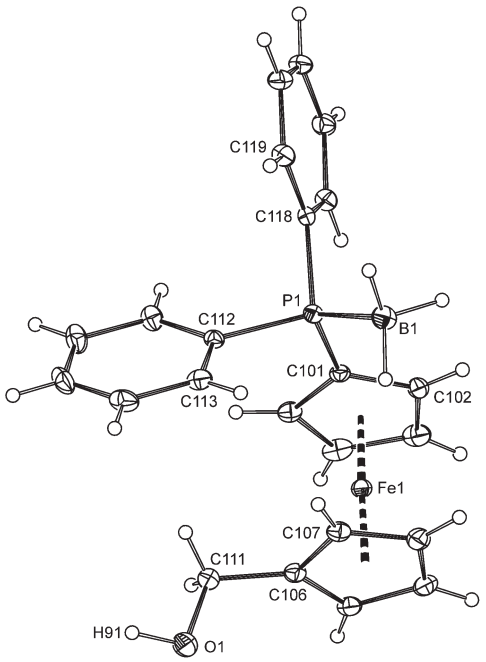

Fig. 1 View of the molecule 1 in the structure of alcohol **5**. Displacement ellipsoids correspond to the 30% probability level. The labelling scheme is analogous in all four crystallographically independent molecules.

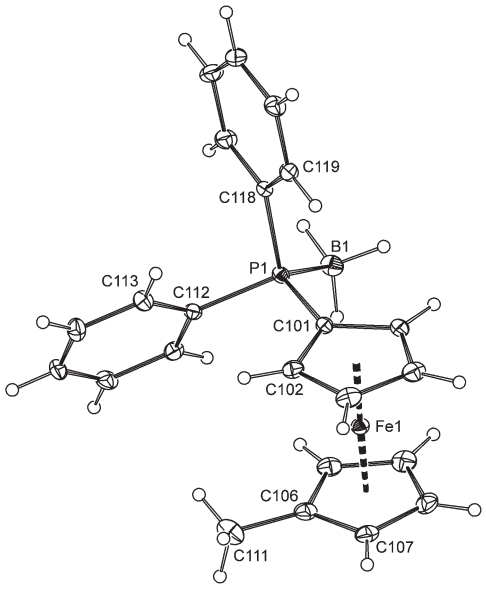

Fig. 2 View of molecule 1 in the crystal structure of adduct **8**. Displacement ellipsoids correspond to the 30% probability level. The labelling of the other three independent molecules is strictly analogous.

introduction of an electron-withdrawing substituent ($PPh_2{\cdot}BH_3$) to the cyclopentadienyl ring.[32] Similar features were observed for (S_p)-**7**, where the Fe–Cg distances differ by *ca.* 0.02 Å. However, the presence of two substituents in adjacent positions results in a twisting at the C1–C2 bond (torsion angle C11–C1–C2–P = 9.3(4)°) and in a slight increase of the tilt angle to 3.2(2)°.

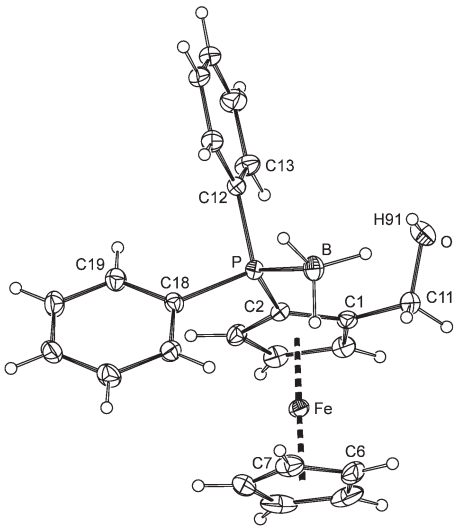

Fig. 3 View of the molecular structure of (S_p)-**7** showing displacement ellipsoids at the 30% probability level. Selected data: Fe–Cg1 1.633(1), Fe–Cg2 1.652(2), P–B 1.930(3), P–C2 1.789(3), P–C12 1.825(3), P–C18 1.817(3), C1–C11 1.498(4), C11–O 1.437(3) Å; ∠Cp1,Cp2 3.2(2), C1–C11–O 111.0(2)°. The ring planes are defined as follows: Cp1 = C(1–5), Cp2 = C(6–10); Cg1 and Cg2 are the respective ring centroids.

Table 1 Selected geometric data for alcohol **5** (in Å and °)[a]

Parameter	Molecule 1	Molecule 2	Molecule 3	Molecule 4
Fe–Cg(P)	1.640(1)	1.642(1)	1.646(1)	1.642(1)
Fe–Cg(C)	1.651(1)	1.645(2)	1.652(1)	1.653(1)
∠Cp(P),Cp(C)	1.8(2)	1.6(2)	2.4(2)	2.2(2)
P–B	1.913(3)	1.924(3)	1.916(3)	1.927(4)
P–C(Cp)	1.791(3)	1.790(3)	1.785(3)	1.786(3)
P–C(Ph)	1.813(3)/ 1.824(3)[b]	1.812(3)/ 1.823(3)[b]	1.807(3)/ 1.817(3)[b]	1.817(3)/ 1.815(3)[b]
C–O	1.436(3)	1.466(7)/ 1.39(1)[c]	1.426(8)/ 1.430(8)[c]	1.436(3)

[a] Cp(P) and Cp(C) stand for the PPh_2- and CH_2OH-substituted cyclopentadienyl rings, respectively. Cg(P) and Cg(C) are the respective ring centroids. [b] Values for two phenyl rings: P*n*–C*n*12/P*n*–C*n*18 (*n* indicates the molecule). [c] Two values due to disorder (two orientations of the CH_2OH moiety).

Table 2 Selected geometric data for compound **8** (in Å and °)[a]

Parameter	Molecule 1	Molecule 2	Molecule 3	Molecule 4
Fe–Cg(P)	1.642(1)	1.640(1)	1.641(1)	1.637(1)
Fe–Cg(C)	1.652(1)	1.651(1)	1.653(1)	1.653(1)
∠Cp(P),Cp(C)	1.3(2)	1.6(2)	2.1(2)	1.3(2)
τ^b	79.0(2)	79.9(2)	78.6(2)	80.3(2)
P–B	1.916(3)	1.921(3)	1.917(3)	1.918(3)
P–C(Cp)	1.782(3)	1.783(3)	1.790(3)	1.788(3)
P–C(Ph)[c]	1.810(2)/ 1.817(3)	1.811(2)/ 1.822(3)	1.815(2)/ 1.822(3)	1.812(2)/ 1.825(3)
C–CH_3	1.495(4)	1.494(4)	1.494(4)	1.507(4)

[a] Cp(P) and Cp(C) denote the phosphine- and methyl-substituted cyclopentadienyl rings, respectively. Cg(P) and Cg(C) are their centroids. [b] Torsion angle C(*n*01)–Cp(P,*n*)–Cp(C,*n*)–C(*n*06). [c] Values for two phenyl rings: P*n*–C*n*12/P*n*–C*n*18 (*n* indicates the molecule).

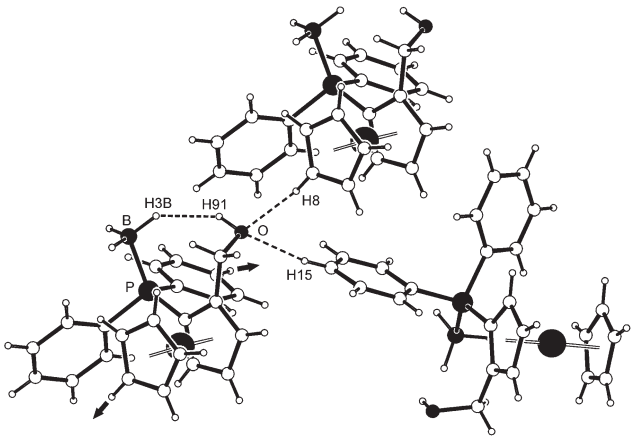

Fig. 4 Intermolecular interactions in the structure of (S_p)-**7**. The arrows indicate where the molecule enters into C–H···O hydrogen bonding interactions as the donor. Hydrogen bond parameters: C8–H8···O^{i}: C8···O^{i} = 3.367(4) Å, angle at H8 = 169°; C15–H15···O^{ii}: C15···O^{ii} = 3.363(4) Å, angle at H15 = 168°; (i) 1 + *x*, *y*, *z*; (ii) 1 − *x*, −1/2 + *y*, 3/2 − *z*.

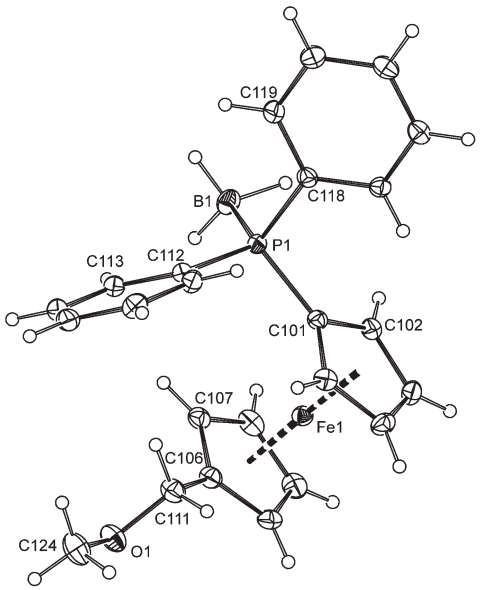

Fig. 5 View of molecule 1 in the structure of **10** with 30% probability displacement ellipsoids. Selected data (Å and °), molecule 1: Fe–Cg(P1) *and* Fe–Cg(C1) 1.649(1), ∠Cp(P1),Cp(C1) 1.0(2); P1–C101 1.788(3), P1–C112 1.818(3), P1–C118 1.811(3), P1–B1 1.919(4), O1–C111 1.418(3), O1–C124 1.428(4); C101–P1–B1 115.4(1), C111–O1–C124 109.7(2); molecule 2: Fe–Cg(P2) 1.649(1), Fe–Cg(C2) 1.651(1), ∠Cp(P2),Cp(C2) 1.6(2); P2–C201 1.787(3), P2–C212 1.808(3), P2–C218 1.817(3), P2–B2 1.915(3), O2–C211 1.417(3), O2–C224 1.429(4); C201–P2–B2 113.6(1), C211–O2–C224 110.0(2). The ring planes are defined as follows: Cp(P*n*) = C(*n*01–*n*05), Cp(C*n*) = C(*n*06–*n*10); Cg(P*n*) and Cg(C*n*) are the respective centroids.

Rather unexpectedly, the crystal assemblies of **5** and (S_p)-**7** do not involve the conventional O–H···O hydrogen bonds that operate, *e.g.*, in the crystal structures of $FcCH_2OH$,[28] **1**,[7] and *rac*-[2-(diphenylphosphino)ferrocen-1-yl]methanol.[29] The molecules of (S_p)-**7** associate only *via* soft C–H···O hydrogen bonds, such that each molecule acts as a double H-bond donor and a double H-bond acceptor (Fig. 4). When combined, these interactions give rise to layers oriented parallel to the *ab* plane.

In addition, the molecules of (S_p)-**7** form intramolecular C–H···Cp-ring π-contacts (C13–H13···Cg1: C13···Cg1 = 3.618(3) Å, angle at H13 = 136°; not indicated in Fig. 4) and intramolecular O1–H91···H3B–B1 *dihydrogen* bonds. In the latter interaction, the negatively charged boron-bound hydrogen (B–H$^{\delta-}$) behaves as a hydrogen bond acceptor for the hydroxyl group within the same molecule (O···H3B = 2.77 Å, O–H91···H3B = 139°). The observed H91···H3B separation (2.00 Å) falls well below a distance corresponding to twice the van der Waals radii of the hydrogen atom (*ca.* 2.2 Å).

It should be noted that dihydrogen bonds[33] involving the BH_3 units as acceptors have been previously studied, predominantly in B–N compounds. However, a survey of the Cambridge Structural Database revealed that even the BH···H–O contacts are relatively common.[34] Most often, they are encountered in the crystal structures of adducts formed from salts with BH_4^- (BH_3CN^-) anions and aminoalcohols.[35] Structures featuring favourable P–BH_3···HO contacts are also quite abundant.[36]

The individual molecules in the structure of **5** also associate into a complicated three-dimensional assembly *via* the relatively weak interactions such as C–H···O and O–H···HB hydrogen bonds, C–H···HB contacts and π–π stacking interactions (see ESI†). The structure thus lacks a principal (*e.g.*, O–H···O) intermolecular interaction favouring a particular orientation of the individual molecules, which in turn results in an increase of the number of structurally independent molecules and disorder of the hydroxymethyl moieties. The crystal packing of **8** is essentially molecular and its isostructural relationship with **5** further corroborates that the strong O–H···O hydrogen bonds, a typical structure-directing force, play a negligible role in the crystal packing of the latter adduct.[37]

The molecular structures of **10** and **11** are depicted in Fig. 5 and 6. Adduct **10** crystallises with triclinic space group $P\bar{1}$ and two virtually identical molecules per asymmetric unit. The corresponding free phosphine **11** crystallises in the common monoclinic space group $P2_1/n$. The compounds share the overall structure: Their cyclopentadienyl rings assume a synclinal eclipsed conformation (τ = 75.1(2)° and 77.1(2)° for molecules 1 and 2 of **10**, and 75.9(1)° for **11**) and exert negligible tilting (below 2°). In both cases, the CH_2OMe arms point to the side of the 'lateral' phenyl group in the phosphine substituent and below the ferrocene unit.

Preparation and characterisation of complexes with ligand 11

Compound **11** is a hybrid and potentially a hemilabile ligand[16] that is closely related to the archetypical phosphinoether donors such as diphenyl(2-methoxymethyl)phosphine[38] or diphenyl[2-(methoxymethyl)phenyl]phosphine[39] and, mainly, to its 'non-spaced' counterpart, $Ph_2PfcOMe$.[40,41] Considering the particular combination of the donor atoms in **11**, the coordination properties of this ligand have been studied towards divalent Group 10 metal ions, ruthenium(II), rhodium(I) and copper(I).

Ru(II) and Rh(I) complexes with auxiliary π-ligands. For screening experiments we chose Ru(II) and Rh(I) precursors

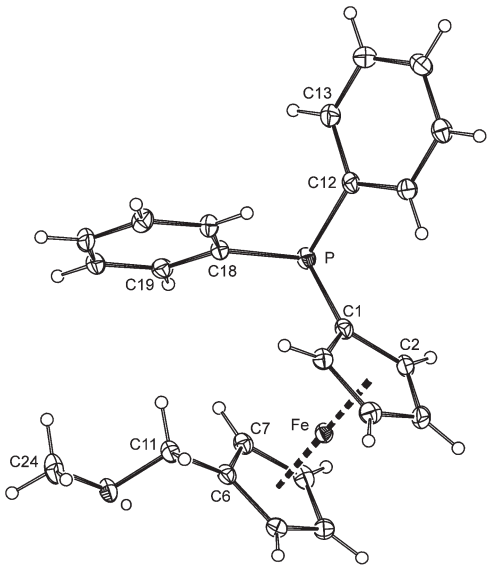

Fig. 6 View of the molecular structure of **11** showing displacement ellipsoids at the 30% probability level. Selected distances and angles (in Å and °): Fe–Cg(P) 1.6433(7), Fe–Cg(C) 1.6482(7), ∠Cp(C),Cp(C) 1.44(9); P–C1 1.814(2), P–C12 1.844(2), P–C18 1.834(2), O–C11 1.430(2), O–C24 1.415(2); O–C11–C6 110.1(1), C11–O–C24 110.7(1). Note: The ring planes are defined as for **10**.

bearing auxiliary π-ligands. Thus, the dimer $[(\eta^6\text{-}p\text{-cymene})RuCl_2]_2$ reacted readily with two molar equivalents of compound **11**, affording the expected bridge-cleavage product **12** in virtually quantitative yield (Scheme 6).

Repeated attempts to prepare an analogous O,P-chelating complex *via* the removal of Ru-bound halide failed. The reaction of **12** with $Ag[SbF_6]$ (in CH_2Cl_2–THF) or with $Na[PF_6]$ (in CH_2Cl_2–methanol) produced only intractable complicated mixtures. Finally, when acetonitrile was employed as the solvent for $Ag[SbF_6]$, the reaction proceeded cleanly to afford the cationic (arene)Ru(II) solvento complex **13** (Scheme 6).

The ^{1}H NMR spectra of **12** and **13** confirm the formulation of these complexes by showing signals due to **11** and the Ru-bound arene. The signal of the coordinated acetonitrile in **13** seen at δ_H 2.13 is split into a doublet with $^5J_{PH}$ of 1.4 Hz.[42] Because of the presence of the stereogenic Ru atom in **13**, the ferrocene protons are diastereotopic and give rise to eight signals in the ^{1}H NMR spectrum. Analogously, the signals due to CH protons at the η^6-arene ligand and the methyl groups of the $CHMe_2$ substituent in **13** are seen as four and two distinct signals, respectively. In contrast, the methylene protons in the remote CH_2OMe pendant are degenerate. The P-coordination of **11** is indicated by a shift of the ^{31}P NMR resonance to a lower field (coordination shift, Δ_P(**12**) = 35.7 ppm). A further shift is seen upon removal of the chloride ligand (Δ_P(**13**) = 46.0 ppm), presumably due to an increased donation to the formed electron-poor Ru^+ centre. Both complexes have been structurally characterised. Their structures are shown in Fig. 7 and 8. Geometric data are given in Table 3.

Both compounds possess the expected three-legged piano stool structure. The interatomic distances as well as the overall geometry of **12** and **13** are similar to those determined earlier for $[(\eta^6\text{-}p\text{-cymene})RuCl_2(Hdpf\text{-}\kappa P)]$[43] and complexes of the type $[(\eta^6\text{-arene})RuCl(PR_3)(MeCN)][PF_6]$,[42] respectively. In both structures, the pseudo-octahedral environments of the Ru(II) centres are distorted, showing dissimilar interligand angles (Cg3–Ru–basal donor >> basal donor–Ru–basal donor). Yet, the dihedral angle subtended by the plane of the η^6-arene ring and the base of the piano stool structure is 3.4(2)° for **12** (basal plane: Cl1, Cl2, P) and 7.2(1)° for **13** (basal plane: Cl, N, P), departing only marginally from 0° expected for an ideal octahedron.

Compound **11** reacted smoothly with dimer $[RhCl(cod)]_2$ (cod = η^2:η^2-cycloocta-1,5-diene) to give phosphine complex **14** (Scheme 7). This complex shows a single ^{31}P NMR resonance

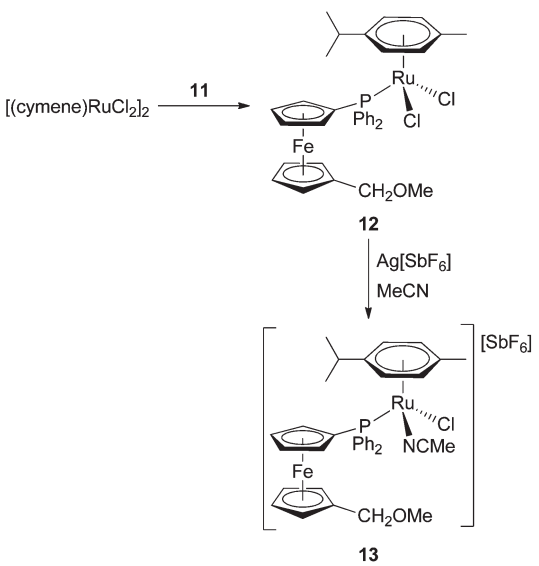

Scheme 6 Preparation of (η^6-*p*-cymene)Ru(II) complexes with ligand **11**.

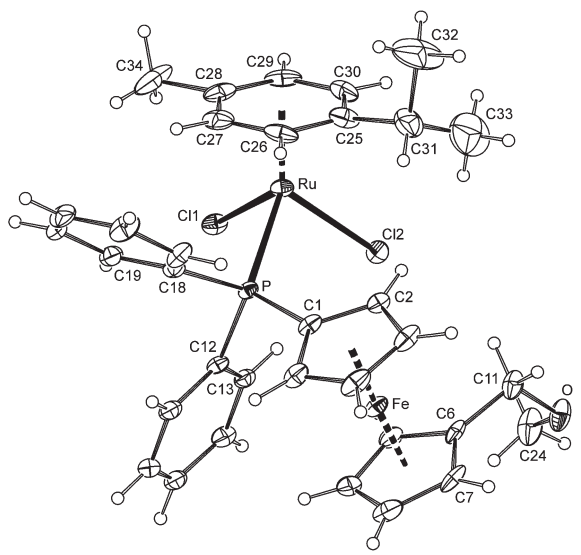

Fig. 7 View of the molecular structure of complex **12**. Displacement ellipsoids correspond to the 30% probability level.

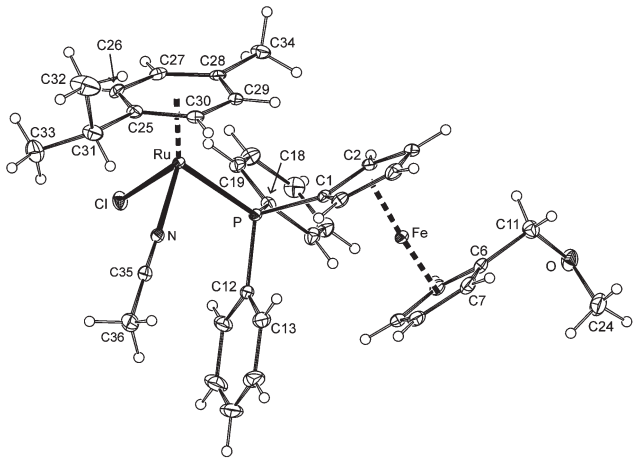

Fig. 8 View of the complex cation in the structure of **13**·1/2$CHCl_3$ showing displacement ellipsoids at the 30% probability level.

Table 3 Selected distances and angles for **12** and **13**·1/2$CHCl_3$ (in Å and °)

Parameter[a]	**12**	**13**[b]
X/Y	Cl1/Cl2	Cl/N
Ru–P	2.364(1)	2.3543(7)
Ru–X	2.407(1)	2.3889(8)
Ru–Y	2.409(1)	2.043(2)
Ru–Cg3	1.714(2)	1.710(1)
P–Ru–X/Y	88.48(5)/87.62(5)	86.61(3)/87.55(7)
X–Ru–Y	88.41(5)	85.48(7)
Cg–Ru–P	128.16(9)	130.96(4)
Cg–Ru–X/Y	122.3(1)/128.1(1)	127.04(5)/124.80(7)
Fe–Cg(P)	1.642(3)	1.642(1)
Fe–Cp(C)	1.647(3)	1.649(2)
∠Cp(P),Cp(C)	2.8(3)	4.6(2)
τ	96.3(4)	137.9(2)

[a] Definitions: Cg(P) and Cg(C) are defined as for **10** (see Fig. 5); τ is the torsion angle C1–Cg(P)–Cg(C)–C6. Cg3 is the centroid of benzene ring C(25–30). [b] Further data: C35–N = 1.132(4), C36–C35–N = 178.8(3).

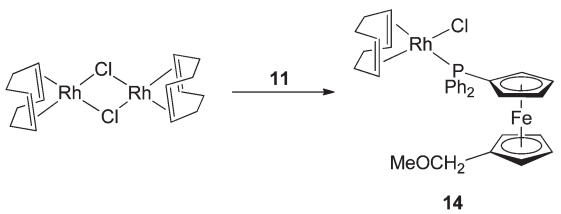

Scheme 7 Preparation of complex **14**.

at δ_P 23.6 (Δ_P(**14**) = 39.9 ppm) split into a doublet due to an interaction with the monoisotopic ^{103}Rh ($^1J_{Rh,P}$ = 151 Hz). The ^{1}H NMR spectrum confirms the presence of a coordinated diene (in an asymmetric environment) and ligand **11**. Attempts to convert **14** into an O,P-chelate or a bridging complex either *via* abstraction of the chloride ligand (with $AgClO_4$) from **14** or directly by the reaction of **11** with $[(cod)Rh(Me_2CO)_2][SbF_6]$[44] produced only ill-defined materials.

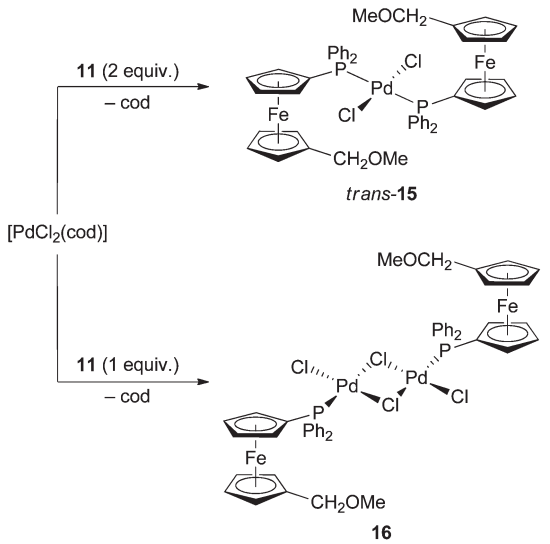

Scheme 8 Preparation of Pd(II) complexes *trans*-**15** and **16**.

Group 10 metal complexes

The attempted reaction of **11** with $[NiCl_2(dme)]$ (dme = 1,2-dimethoxyethane) did not afford any defined product, very likely due to a low (solvolytic) stability of 'complexes' arising in this system. On the other hand, reactions of phosphine **11** with $[PdCl_2(cod)]$ as a precursor of the softer 'MCl_2' fragment (Scheme 8) proceeded cleanly and produced two different phosphine complexes depending on the reaction stoichiometry: the diphosphine complex *trans*-**15** at a 2 : 1 ligand-to-metal ratio, and the symmetric, chloride-bridged dimer **16** when the starting materials were mixed in equimolar amounts.

The removal of chloride ligand(s) from complex *trans*-**15** by one or two equivalents of $AgClO_4$ led to poorly defined, non-crystallising violet materials. As an alternative approach to the elusive O,P-chelate complex, ligand **11** was reacted with $[Pd(MeCN)_4][BF_4]_2$ as a stable and defined Pd(II) source devoid of firmly bound auxiliary donors.[45] Treatment of $[Pd(MeCN)_4][BF_4]_2$ with **11** (2 equiv.) in $CDCl_3$ proceeded under the liberation of MeCN (δ_H 1.99) to afford a deep blue-violet product, showing extremely broad NMR signals.[46] Evaporation of the reaction mixture afforded a violet glassy solid, which unfortunately defied all attempts at purification by crystallisation.

When $[Ph_4As]Cl$ in excess was added to the reaction mixture, a marked colour change from deep violet to red-orange occurred immediately, reflecting the formation of the dichloride complex *trans*-**15**, which was evidenced by the ^{1}H and ^{31}P NMR spectra.[47]

Although no defined product could be isolated from the reaction between **11** and $[Pd(MeCN)_4][BF_4]_2$, the overall reaction course can be rationalised as shown in Scheme 9. In the first step, phosphine **11** replaces the acetonitrile ligands to give a fluxional cationic species of the type $\{Pd(\mathbf{11})_2\}^{2+}$ or its analogue stabilised through a weak coordination of the solvent or the counter anion. This intermediate readily takes up free

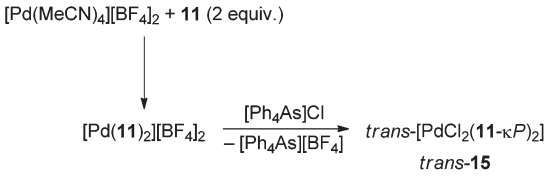

Scheme 9 Stepwise formation of *trans*-**15** from $[Pd(MeCN)_4][BF_4]_2$, **11** and $[Ph_4As]Cl$.

chloride ions to afford the stable diphosphine complex *trans*-**15** *via* replacement of the ligand's oxygen or weakly bound supporting ligands.

Analogous reactions with $[PtCl_2(cod)]$ proceeded in a different manner. The reaction of $[PtCl_2(cod)]$ with **11** at a Pt–P molar ratio of 1 : 1 in $CDCl_3$ produced a mixture containing unreacted $[PtCl_2(cod)]$, diphosphine complex *cis*-$[PtCl_2(\mathbf{11}\text{-}\kappa P)_2]$ (*cis*-**17**; δ_P 9.8, $^1J_{Pt,P}$ = 3759 Hz) and liberated cod in equal molar ratios, according to the NMR analysis. In addition to these rather expected products, another Pt(II)–**11** species was also seen, albeit in tiny amounts (δ_P 11.5, $^1J_{Pt,P}$ = 2622 Hz). When the amount of the ligand was increased to two equivalents (Pt–P = 1 : 2), the reaction gave rise to a mixture of *cis*-**17** and liberated cod. Even in this case, however, the mentioned side product was detected in the reaction mixture, corresponding to *ca.* 3 mol% of the total Pt(II). Notably, the amount of the side product increased slowly after the addition of excess **11** either directly during mixing of the starting materials or later to the reaction mixture. Crystallisation of the reaction solution by diffusion of diethyl ether afforded a mixture of small plate-like crystals of *cis*-**17**[48] and bar-like crystals of the other (minor) product, which was unambiguously identified as *trans*-**17** by X-ray crystallography.

The observed behaviour corresponds with kinetic inertness of Pt(II), which prevents the formation of the thermodynamically favoured *trans*-isomer from $[PtCl_2(cod)]$. Conversion of *cis*-**17** (the kinetic product) to *trans*-**17** proceeds *via* an associative pathway and is therefore facilitated in the presence of free **11**.[49]

Complexes *trans*-**15**, **16** and *trans*-**17** were structurally characterised by X-ray diffraction analysis. Compounds *trans*-**15** and *trans*-**17** are isostructural and, hence, only the structure of the former complex is shown in Fig. 9 along with data for both compounds. A view of the molecular structure of *trans*-**17** is available as ESI (Fig. S3†).

Complexes *trans*-**15** and *trans*-**17** crystallise with an imposed symmetry (the central atoms reside on crystallographic inversion centres), which renders only the half of their molecules structurally independent and the coordination spheres exactly planar. Their structures are similar to those of *trans*-$[MCl_2(Hdpf\text{-}\kappa P)_2]\cdot 2AcOH$ (M = Pd, Pt)[50] and Pd(II) complexes featuring P-monodentate, 1′-substituted (diphenylphosphino)-ferrocene donors, *trans*-$[MCl_2(Ph_2PfcY\text{-}\kappa P)_2]$.[51] Unlike these compounds, however, the chloride ligands in *trans*-**15** and *trans*-**17** are disordered over two positions related by rotation of the Pt–Cl bonds along the P–P′ axis (relative populations: *ca.* 70 : 30). This feature may well reflect the mobility of the monoatomic ligands (though limited) within the empty space defined by the bulky phosphinoferrocene ligands. The ferrocene moieties in *trans*-**15** and *trans*-**17** show tilt angles of *ca.* 3° and adopt intermediate conformations close to synclinal eclipsed ($\tau \approx 82°$).

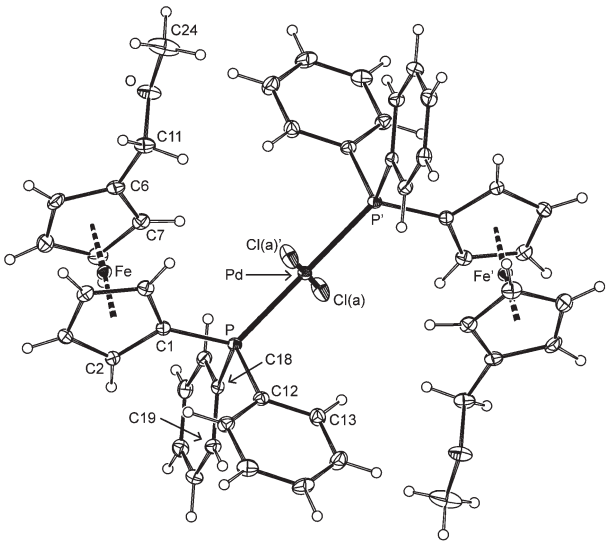

Fig. 9 View of the molecular structure of *trans*-**15** showing displacement ellipsoids at the 30% probability level and only one position of the disordered Cl atom. Prime-labelled atoms are generated by crystallographic inversion. Selected distances and angles (in Å and °; parameters for *trans*-**17** are given in square brackets): M–P 2.3408(5) [2.3220(5)], M–Cl(a/b) 2.254(3)/2.313(2) [2.261(4)/2.317(2)], P–M–Cl(a/b) 94.6(1)/90.53(6) [90.2(1)/94.51(5)].

The crystal structure of the dipalladium complex **16** is presented in Fig. 10. Even this complex crystallises with an imposed crystallographic symmetry, such that the centre of the Pd_2Cl_2 core coincides with the crystallographic inversion centre. Palladium and its four ligating atoms (P, Cl1, Cl2 and Cl2′) in **16** are coplanar within *ca.* 0.06 Å. The Pd–Cl distance involving Cl1 as a terminal donor is expectedly shorter than for the bridging chlorides Cl2/2′, which are bonded somewhat asymmetrically. The relative bulkiness of the phosphine donor as compared to the monoatomic chloride donors is nicely reflected by the interligand angles, decreasing in the order P–Pd–Cl2 > P–Pd–Cl1 > Cl2–Pd–Cl2′ > Cl1–Pd–Cl2′. Similar structural features are observed for $[PdCl(\mu\text{-}Cl)(Ph_2PfcPO_3Et_2\text{-}\kappa P)]_2$.[51c]

The reaction of 11 with copper(I) triflate

In addition to the Group 8–10 metals, the coordination study with **11** was extended to Cu(I), which has a significant hard-soft borderline character.[52] Mixing ligand **11** (2 equiv.) with copper(I) triflate (as a toluene adduct) in dry $CDCl_3$ afforded a yellow solution, containing a single Cu-**11** product according to ^{31}P NMR analysis (δ_P −7.7). Unfortunately, the ^1H NMR spectra were rather inconclusive as they displayed extremely broad signals for the ferrocene CH and methylene protons. Signals of the methoxy (δ_H 3.03) and the PPh_2 groups were also

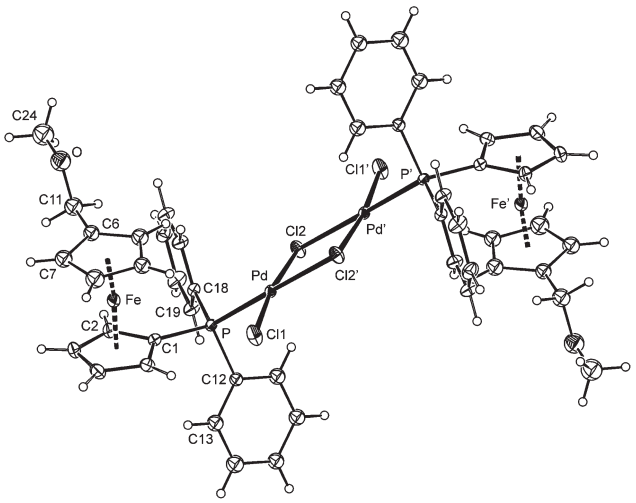

Fig. 10 View of the molecular structure of **16** showing 30% probability displacement ellipsoids. For clarity, only one orientation of the disordered rings C(6–10) and C(12–17) is shown. Primed atoms are generated by the crystallographic inversion. Selected distances and angles (in Å and °): Pd–Cl1 2.2621(10), Pd–Cl2 2.3281(8), Pd–Cl2′ 2.4300(9), Pd–P 2.2294(8); P–Pd–Cl1 91.64(3), P–Pd–Cl2 93.69(3), Cl1–Pd–Cl2 89.25(3), Cl2–Pd–Cl2′ 85.30(3).

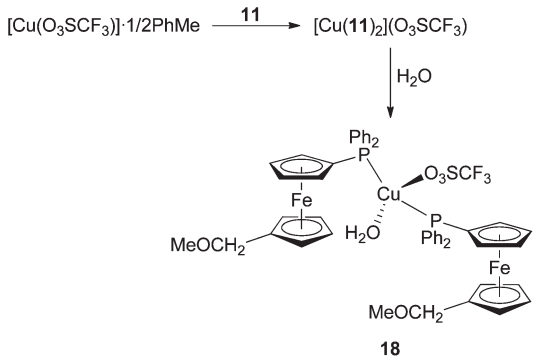

Scheme 10 Formation of **18** from $[Cu(O_3SCF_3)]\cdot 1/2PhMe$ and **11**.

broadened, but to a lesser extent. Evaporation of the reaction mixture followed by the addition of commercial (wet) diethyl ether and storing overnight at 4 °C afforded aqua complex **18** as a yellow crystalline solid (Scheme 10).

The ^{1}H NMR spectrum of **18** showed the expected signals due to coordinated **11**; the ^{31}P NMR signal (δ_P −7.8) was observed close to that of the presumed intermediate $[Cu(\mathbf{11})_2](O_3SCF_3)$. In its ESI mass spectrum, compound **18** displayed a signal at m/z 891, corresponding to $[Cu(\mathbf{11})_2]^+$ as the heaviest fragment species, whereas the IR spectra confirmed the presence of the triflate anion (1290, 1229 and 1026 cm^{-1})[53] and water.

Similar to the complexes mentioned above, the methoxymethyl group in complex **18** behaves as an innocent dangling substituent. This was indeed corroborated by X-ray diffraction analysis (Fig. 11 and Table 4).

The Cu(I) ion in complex **18** possesses a relatively common P_2O_2 donor set (for a detailed view, see ESI, Fig. S4†).

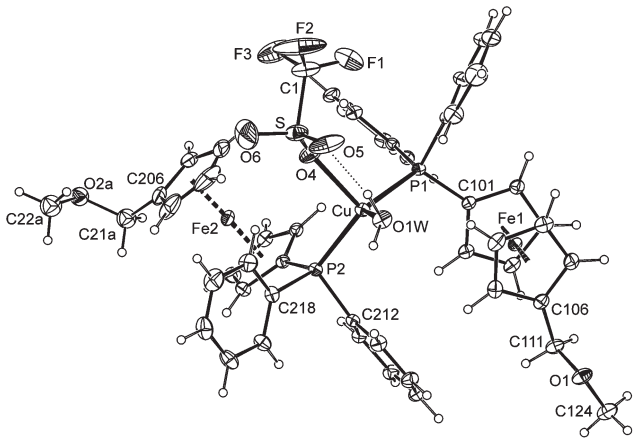

Fig. 11 View of the molecular structure of complex **18** showing atom labelling and displacement ellipsoids at the 30% probability level. For clarity, only one orientation of the disordered methoxymethyl group in ligand 2 (Fe2) is shown. The intramolecular hydrogen bond O1W–H2W···O5 is indicated by a dotted line (O1W···O5 = 2.807(1) Å).

Table 4 Selected distances and angles for complex **18** (in Å and °)[a]

Distances		Angles	
Cu–P1	2.2527(9)	P1–Cu–P2	129.27(4)
Cu–P2	2.247(1)	P1–Cu–O4	104.92(4)
Cu–O4	2.2616(9)	P1–Cu–O1W	111.53(4)
Cu–O1W	2.149(1)	P2–Cu–O4	103.68(4)
S–O (range)	1.422(1)–1.439(1)	P2–Cu–O1W	110.64(4)
S–C1	1.818(1)	O4–Cu–O1W	87.65(4)
Fe1–Cp(P1)	1.644(2)	∠Cp(P1), Cp(C1)	2.4(2)
Fe1–Cp(C1)	1.643(2)	∠Cp(P2), Cp(P2)	2.2(3)
Fe2–Cp(P2)	1.643(2)	τ_1	145.9(3)
Fe2–Cp(C2)	1.643(2)	τ_2	140.8(4)

[a] Definitions of the ring planes: Cp(Pn) = C(n01–n05), Cp(Cn) = C(n06–n10). Cg$^{P/C}$ are the respective centroids. τ_n is the torsion angle C(n01)–Cg(Pn)–Cg(Cn)–C(n06).

Nonetheless, there is only a handful of such Cu(I) complexes bearing phosphine *and* ether or aqua ligands that have been structurally characterized,[54] namely $[Cu(PPh_3)_2(THF\text{-}\kappa O)(O_3SCF_3\text{-}\kappa O)]$[55] and a dicopper(I) complex with an extended, calixarene-type ligand.[56] The Cu–P bond lengths in **18** are similar to each other and also to the Cu–PPh_3 distances in $[Cu(PPh_3)_2(THF\text{-}\kappa O)(O_3SCF_3\text{-}\kappa O)]$. In contrast, the individual Cu–O distances differ significantly from each other (Cu–O1W < Cu–O4), reflecting very likely the different donor abilities of the triflate ion and water present as O-donors in **18** (*cf.* Cu–O(triflate) 2.168(2), Cu–O(THF) 2.125(2) Å in the reference compound). The donor atoms in **18** constitute a distorted tetrahedral environment in which the P–Cu–P angle is the most open and the O–Cu–O angle is the most acute (Fig. S4†). This distortion seems to result not only from different steric demands of the ligands, but also from an intramolecular hydrogen-bonding interaction O1W–H12W···O5, which results in inclination of O1W towards the coordinated triflate. The other hydrogen atom (H1W) in the Cu-bound water molecule forms a hydrogen bridge to ether oxygen (O1) in a neighbouring

molecule, which in turn results in the formation of molecular pairs lying around crystallographic inversion centres (see ESI, Fig. S5†).

Conclusions

The reduction of ferrocenecarbaldehydes bearing phosphine substituents at position 1′ or 2 with an excess of BH_3·L (L = THF or SMe_2) in THF at 0 °C proceeds selectively to afford stable phosphinoalcohol–borane adducts in quantitative yields. In contrast, a similar reduction performed at elevated temperatures (refluxing in THF) produces methylferrocene derivatives resulting from the exhaustive reduction (deoxygenation) of the starting phosphino-aldehydes. The observed difference in the reaction course emphasises the need for careful optimisation of the reaction conditions in reductions with borane which, on the other hand, may pay off by the highly selective preparation of chemically different compounds.

Importantly, the resulting phosphinoalcohol–borane adducts represent stable, protected-at-phosphorus synthetic building blocks suitable for the preparation of other phosphinoferrocenyl derivatives. With this study, we have demonstrated their synthetic potential by the smooth, two-step preparation of phosphinoether donor **11** from **5**. Compound **11** extends the still narrow family of donors formally homologous to the known functional phosphinoferrocene ligands ($Ph_2PfcY \rightarrow Ph_2PfcCH_2Y$, ref. 6*e–j*).

The coordination study with **11** clearly demonstrated flexibility as well as the hybrid and potentially hemilabile nature of this donor. The presence of a methylene spacer in **11** renders the ligand structure more flexible and requires the formation of large chelate rings, which both lower the tendency towards the formation of stable chelates. If formed, the chelate rings seem to readily open in the presence of suitable donors such as Cl^- and adventitious H_2O. The behaviour of **11** thus contrasts with that of $Ph_2PfcOMe$, in which chelate coordination is facilitated by a more rigid pre-disposition of the donor moieties.

Experimental

Materials and methods

The syntheses were carried out under an argon atmosphere and with the exclusion of direct sunlight. Tetrahydrofuran (THF) was distilled from potassium/benzophenone ketyl. Solvents used for work-up and chromatography (Lachner) were used without any further purification. 1,1′-Dibromoferrocene,[57] **2**,[7] (S_p)-**4**,[11b] $[(\eta^6\text{-}p\text{-cymene})RuCl_2]_2$,[58] and $[MCl_2(cod)]$ (M = Pd, Pt)[59] were prepared as described in the literature. Other chemicals (including anhydrous acetonitrile, dimethylsulphoxide and dichloromethane) were used as received from commercial sources (Sigma-Aldrich).

NMR spectra were recorded with a Varian Unity Inova 400 spectrometer at 25 °C. Chemical shifts (δ/ppm) are given relative to internal $SiMe_4$ (^{13}C and ^1H) or to external 85% aqueous H_3PO_4 (^{31}P). In addition to the usual notation of signal multiplicity, vt and vq were used to distinguish virtual triplets and quartets due to AA′BB′ and AA′BB′X spin systems arising from the ferrocene cyclopentadienyls (A, B = ^1H, X = ^{31}P). IR spectra were recorded on an FT IR Nicolet Magna 650 spectrometer. Electron impact ionisation (EI) mass spectra including high-resolution measurements (HR) were obtained with a GCT Premier spectrometer (Waters). Electrospray ionisation (ESI) mass spectra were recorded with a LCQ Fleet (Thermo Fisher Scientific; HR) or an Esquire 3000 (Bruker; low resolution) spectrometer.

Syntheses

Reaction tests with aldehyde 2. Aldehyde **2** (100 mg, 0.25 mmol) was dissolved in dry THF (5 mL) and the solution was cooled if required. The appropriate BH_3 source (1 mmol) was added and the resulting mixture was treated as specified below. In all cases, the addition of BH_3 resulted in a swift colour change from the original reddish-orange to orange-yellow. Upon completion of the reaction, the mixture was cooled to room temperature when necessary, treated with methanol (1 mL, stirring for 30 min) to destroy any unreacted borane and then evaporated under vacuum. The product(s) were isolated by column chromatography over silica gel using ethyl acetate–hexane (2 : 1) as the eluent.

The reduction of **2** with BH_3·THF (1 M in THF, 1.0 mL, 1.0 mmol) at 0 °C (ice bath) for 90 min afforded pure **5** (97 mg, 93%). A tiny amount of $FcPPh_2$·BH_3 (*ca.* 5 mg) was easily removed during chromatography as the first band. The reaction was performed several times with different lots of the borane solution (1 M BH_3 in THF stabilised with 0.005 M $NaBH_4$, all from Sigma-Aldrich) without any noticeable change. Increasing the reaction temperature to *ca.* 23 °C did not change the reaction course (isolated yield of **5**: 95 mg, 92%). The reduction with BH_3·SMe_2 (1 M in THF, 1.0 mL, 1.0 mmol) at 0 °C gave the same product (isolated yield of **5**: 94 mg, 91%).

In another series of experiments, the reducing agent was added at room temperature and the mixture was immediately transferred to a preheated oil bath and refluxed overnight (16 h). The reaction with BH_3·THF (1 M in THF, 1.0 mL, 1.0 mmol) under reflux furnished a mixture of two products that were easily separated by column chromatography. The first (faster eluting) band contained **8** (57 mg, 57%; contaminated with $FcPPh_2$·BH_3), while the second was found to contain pure phosphinoalcohol–borane adduct **5** (41 mg, 39%). When the reaction was repeated, the products were isolated in different amounts (67 mg of crude **8**, 27 mg (26%) of **5**). A similar reduction with BH_3·SMe_2 (1 M in THF, 1.0 mL, 1.0 mmol; refluxing/16 h) afforded a yellow solid, which gave only one band during the chromatographic purification. Subsequent evaporation afforded **8** in quantitative yield (100 mg). According to NMR analysis, the product was contaminated with traces of $FcPPh_2$·BH_3. The compound was crystallised from hot heptane.

Analytical data for 5. ^{1}H NMR ($CDCl_3$): δ *ca.* 0.75–1.80 (very br m, 3 H, BH_3), 1.45 (t, $^{3}J_{HH}$ = 6.0 Hz, 1 H, CH_2OH), 4.07 (vt, J' = 1.9 Hz, 2 H, $C_5H_4CH_2OH$), 4.12 (d, $^{3}J_{HH}$ = 6.0 Hz, 2 H, CH_2OH), 4.22 (vt, J' = 1.9 Hz, 2 H, $C_5H_4CH_2OH$), 4.42 (vq, J' = 1.9 Hz, 2 H, $C_5H_4PPh_2$), 4.53 (m, 2 H, $C_5H_4PPh_2$), 7.38–7.50 (m, 8 H, PPh_2), 7.54–7.62 (m, 2 H, PPh_2). Note: the signals due to CH_2OH collapse into unresolved broad signals when the solution is allowed to stand for some time. $^{13}C\{^{1}H\}$ NMR ($CDCl_3$): δ 60.18 (CH_2OH), 69.36 (d, $^{1}J_{PC}$ = 68 Hz, C–P of $C_5H_4PPh_2$), 69.52 and 70.01 (2 × s, 2 C, CH of $C_5H_4CH_2OH$); 72.16 (d, J_{PC} = 7 Hz, 2 C, CH of $C_5H_4PPh_2$), 73.13 (d, J_{PC} = 10 Hz, 2 C, CH of $C_5H_4PPh_2$), 89.47 (s, *C*-CH_2OH of $C_5H_4CH_2OH$), 128.46 (d, J_{PC} = 10 Hz, 4 C, CH of PPh_2), 130.97 (d, J_{PC} = 2 Hz, 2 C, CH of PPh_2), 131.07 (d, $^{1}J_{PC}$ = 59 Hz, 2 C, C_{ipso} of PPh_2), 132.60 (d, J_{PC} = 10 Hz, 4 C, CH of PPh_2). $^{31}P\{^{1}H\}$ NMR ($CDCl_3$): δ 16.6 (br d). IR (Nujol): ν/cm^{-1} 3576 w, 3539 m, 2403 s, 2366 s, 2341 m, 1308 m, 1230 m, 1181 m, 1172 s, 1109 s, 1056 vs, 1026 s, 997 vs, 920 w, 846 m, 840 s, 821 s, 745 vs, 704 vs, 642 s, 623 w, 611 m, 529 m, 519 m, 499 vs, 479 s, 466 m, 442 m. ESI+ MS: *m*/*z* 439 (probably $[M + K - BH_3]^+$), 437 (dominant; $[M + Na]^+$), 400 ($[M - BH_3]^+$). MS (EI): *m*/*z* (relative abundance): 414 (2, $M^{+\cdot}$), 401 (5), 400 (20, $[M - BH_3]^{+\cdot}$), 385 (11), 384 (46, $[M - BH_3 - O]^{+\cdot}$), 307 (11), 226 (8), 169 (5), 170 (5), 167 (100), 165 (22), 152 (5), 121 (3, $[C_5H_5Fe]^+$), 56 (5, Fe^+). HR MS (EI) calc. for $C_{23}H_{24}{}^{11}B^{56}FeOP$ ($M^{+\cdot}$) 414.1007; found 414.1018. Anal. calc. for $C_{23}H_{24}BFeOP$ (414.1): C 66.71, H 5.84%. Found: C 66.41, H 5.92%.

Analytical data for 8. ^{1}H NMR ($CDCl_3$): δ *ca.* 0.75–1.80 (very br m, 3 H, BH_3), 1.73 (s, 3 H, CH_3), 3.94 (vt, J' = 1.9 Hz, 2 H, C_5H_4), 4.04 (vt, J' = 1.8 Hz, 2 H, C_5H_4), 4.31 (vq, J' = 1.9 Hz, 2 H, C_5H_4), 4.44 (m, 2 H, C_5H_4), 7.37–7.49 (m, 8 H, PPh_2), 7.55–7.62 (m, 2 H, PPh_2). $^{13}C\{^{1}H\}$ NMR ($CDCl_3$): δ 14.15 (s, CH_3), 68.56 (d, $^{1}J_{PC}$ = 70 Hz, C–P of $C_5H_4PPh_2$), 69.15 and 70.90 (2 × s, 2 C, CH of $C_5H_4CH_3$); 72.72 (d, J_{PC} = 7 Hz, 2 C, CH of $C_5H_4PPh_2$), 73.41 (d, J_{PC} = 10 Hz, 2 C, CH of $C_5H_4PPh_2$), 85.61 (s, *C*-CH_3 of $C_5H_4CH_3$), 128.35 (d, J_{PC} = 10 Hz, 4 C, CH of PPh_2), 130.77 (d, J_{PC} = 2 Hz, 2 C, CH of PPh_2), 131.51 (d, $^{1}J_{PC}$ = 59 Hz, 2 C, C_{ipso} of PPh_2), 132.65 (d, J_{PC} = 9 Hz, 4 C, CH of PPh_2). $^{31}P\{^{1}H\}$ NMR ($CDCl_3$): δ 16.6 (br d). Anal. calc. for $C_{23}H_{24}BFeOP$ (398.1): C 69.40, H 6.08%. Found: C 69.54, H 5.93%.

Preparation of 1′-(diphenylphosphino)-1-hydroxymethylferrocene–borane (1/1) (5). A solution of BH_3·THF (12 mL of 1.0 M in THF, 12 mmol; Sigma-Aldrich, stabilised with 0.005 M $NaBH_4$) was added to a solution of **1** (1.995 g, 5.0 mmol) in dry THF (25 mL) with stirring and cooling in an ice bath. Upon mixing, the colour of the reaction mixture quickly turned from the original red-orange to deep orange-yellow. After stirring at 0 °C for 90 min, the reaction mixture was diluted with wet diethyl ether (5 mL of ether + 0.5 mL of H_2O) to decompose an excess of borane, stirred for another 30 min and evaporated. The orange residue was dissolved in a small volume of warm ethyl acetate and introduced to the top of a silica gel column. Elution with ethyl acetate–hexane (2 : 1) led to the development of two bands. The first minor band containing predominantly $FcPPh_2$·BH_3 was discarded. The second orange-yellow band was collected and evaporated under vacuum to afford analytically pure adduct **5** as an orange microcrystalline solid. Yield: 1.838 g (89%). If appropriate, the compound can be crystallised from hot heptane or warm ethyl acetate–hexane.

1′-(Dicyclohexylphosphino)-1-hydroxymethylferrocene–borane (1/1) (6). Compound **6** was obtained from aldehyde **3** (1.240 g, 3.0 mmol in 30 mL of THF) and BH_3·THF (7.5 mL of 1.0 M in THF, 7.5 mmol) as described above for **5**. The resulting crude material was purified by chromatography on silica (packed in hexane–diethyl ether, 1 : 1). Hexane was used first to elute non-polar impurities and then replaced with hexane–diethyl ether (1 : 1) to elute the major band due to the product. Subsequent evaporation and drying under vacuum afforded pure **6** as an orange microcrystalline solid. Yield: 1.238 g (97%).

^{1}H NMR ($CDCl_3$): δ *ca.* 0.15–1.10 (very br m, 3 H, BH_3), 1.08–2.03 (m, 23 H, Cy and OH), 4.25 (vt, $J' \approx$ 1.8 Hz, 2 H, $C_5H_4CH_2OH$), 4.31 (vq, $J' \approx$ 1.8 Hz, 2 H, $C_5H_4PCy_2$), 4.35 (vt, $J' \approx$ 1.9 Hz, 2 H, $C_5H_4CH_2OH$), 4.41 (d, $^{3}J_{HH}$ = 5.6 Hz, 2 H, CH_2OH), 4.43 (d of vt, $J \approx$ 1.0, 1.9 Hz, 2 H, $C_5H_4PCy_2$). $^{13}C\{^{1}H\}$ NMR ($CDCl_3$): δ 25.91 (d, J_{PC} = 2 Hz, CH_2 of Cy), 26.81 (s, CH_2 of Cy), 26.83 (d, $J_{PC} \approx$ 3 Hz, CH_2 of Cy), 26.93 (d, J_{PC} = 5 Hz, CH_2 of Cy), 27.09 (d, J_{PC} = 3 Hz, CH_2 of Cy), 32.27 (d, $^{1}J_{PC}$ = 35 Hz, α-CH of Cy), 60.41 (CH_2OH), 68.58 (d, $^{1}J_{PC}$ = 56 Hz, C–P of $C_5H_4PPh_2$), 69.27 and 70.04 (2 × s, 2 C, CH of $C_5H_4CH_2OH$); 70.81 and 72.30 (2 × d, J_{PC} = 7 Hz, 2 C, CH of $C_5H_4PPh_2$); 89.76 (s, *C*-CH_2OH of $C_5H_4CH_2OH$). $^{31}P\{^{1}H\}$ NMR ($CDCl_3$): δ 24.0 (br d). IR (Nujol): ν/cm^{-1} 3579 s, *ca.* 3200–3535 s (maximum at 3431), 2370 vs, 2340/2333 s, 2250 m, 1311 w, 1296 w, 1275 w, 1253 w, 1202 m, 1168 s, 1062 vs, 1049/1043 s, 1030/1024 m, 1007 w, 981 m, 920 m, 890 m, 850 s, 838 s, 819 s, 763/758 s, 633 s, 605 s, 528 s, 507 s, 497 m, 464 m. MS (EI): *m*/*z* (relative abundance) 426 (4, $M^{+\cdot}$), 413 (12), 412 (68, $[M - BH_3]^{+\cdot}$), 410 (8), 397 (35), 396 (100, $[M - BH_3 - O]^{+\cdot}$), 394 (10), 330 (7), 329 (27), 314 (14), 313 (43), 312 (5), 311 (6), 232 (31), 231 (100), 230 (9), 229 (25), 201 (5), 200 (32), 199 (28), 198 (8), 186 (23), 167 (5), 153 (5), 152 (18), 151 (13), 135 (34), 134 (20), 133 (5), 121 (36, $[C_5H_5Fe]^+$), 79 (10, Fe^+), 67 (5), 56 (13). HR MS (EI) calc. for $C_{23}H_{36}{}^{11}B^{56}FeOP$ ($M^{+\cdot}$) 426.1946; found 426.1933. Anal. calc. for $C_{23}H_{36}BFeOP$ (426.1): C 64.82, H 8.52%. Found: C 65.01, H 8.55%.

(S_p)-2-(Diphenylphosphino)-1-hydroxymethylferrocene–borane (1/1) [(S_p)-7]. An ice-cooled solution of (S_p)-**4** in dry THF (100 mg, 0.25 mmol in 5 mL) was treated with a solution of BH_3 in the same solvent (1.0 mL, 1.0 M, 1.0 mmol). The mixture immediately turned from orange to yellow. After stirring at 0 °C for 90 min, the reaction mixture was quenched with methanol (0.5 mL), diluted with diethyl ether and evaporated under vacuum. The orange-yellow glassy residue was purified by column chromatography on silica gel with diethyl ether. Evaporation of a single yellow band followed by drying under vacuum afforded pure (S_p)-**7** as a yellow-orange glassy solid. Yield: 104 mg (quant.). When appropriate, the adduct can be re-crystallised from hot heptane. However, such crystallisation is accompanied by a significant loss of the material and the compound often separates as an amorphous solid.

^{1}H NMR ($CDCl_3$): δ *ca.* 0.95–2.00 (very br m, 3 H, BH_3), 1.94 (t, $^3J_{HH}$ = 6.9 Hz, 1 H, CH_2OH), 3.92 (m, 1 H, C_5H_3), 4.20 (s, 5 H, C_5H_5), 4.31 (dd, $^2J_{HH}$ = 12.8, $^3J_{HH} \approx$ 6.5 Hz, 1 H, CH_2OH), 4.41 (t, J = 2.9 Hz, 1 H, C_5H_3), 4.61 (m, 1 H, C_5H_3), 4.71 (dd, $^2J_{HH}$ = 12.8, $^3J_{HH} \approx$ 6.8 Hz, 1 H, CH_2OH), 7.32–7.58 (m, 8 H, PPh_2), 7.66–7.74 (m, 2 H, PPh_2). $^{13}C\{^1H\}$ NMR ($CDCl_3$): δ 59.28 (CH_2OH), 68.45 (d, $^1J_{PC}$ = 64 Hz, C–P of C_5H_3), 70.17 (s, C_5H_5), 70.43 (d, J_{PC} = 6 Hz, CH of C_5H_3), 73.88 (d, J_{PC} = 4 Hz, CH of C_5H_3), 74.09 (d, J_{PC} = 7 Hz, CH of C_5H_3), 92.22 (d, $^2J_{PC}$ = 15 Hz, *C*-CH_2OH of C_5H_3), 128.39 and 128.53 (2 × d, 2 C, J_{PC} = 10 Hz, CH of PPh_2); 130.23 (d, $^1J_{PC}$ = 61 Hz, C_{ipso} of PPh_2), 130.91 and 131.23 (2 × d, J_{PC} = 2 Hz, CH of PPh_2); 131.31 (d, $^1J_{PC}$ = 59 Hz, C_{ipso} of PPh_2), 132.37 and 133.25 (2 × d, J_{PC} = 9 Hz, 2 C, CH of PPh_2). $^{31}P\{^1H\}$ NMR ($CDCl_3$): δ 15.4 (br d). IR (neat): ν/cm^{-1} *ca.* 3430 very br m, 3077 w, 3057 w, 3006 w, 2392 s, 2352 sh, 2261 w, 1484 m, 1436 s, 1411 w, 1315 composite br, 1249 m, 1186 m, 11 621 m, 1107 s, 1061 s, 1000 m, 825 s, 742 s, 699 s, 649 m, 636 m, 611 m, 495 s, 478 s. MS (EI): *m*/*z* (relative abundance) 414 (6, $M^{+\cdot}$), 400 (100, $[M - BH_3]^{+\cdot}$), 384 (37), 279 (11), 199 (8), 173 (42, $[PPh_2 - 2H]^+$), 171 (7), 170 (6), 153 (7), 152 (9), 138 (9), 121 (51, $[C_5H_5Fe]^+$), 108 (14). HR MS (EI) calc. for $C_{23}H_{24}{}^{11}B^{56}FeOP$ ($M^{+\cdot}$) 414.1007; found 414.0997. Anal. calc. for $C_{23}H_{24}BFeOP$ (414.1): C 66.71, H 5.84%. Found: C 66.66, H 6.00%.

Deborylation of 5. Adduct **5** (10.5 mg, 0.025 mmol) and 1,4-diazabicyclo[2.2.2]octane (3.5 mg, 0.03 mmol) were dissolved in C_6D_6 (*ca.* 0.7 mL) and the solution was warmed to 60 °C for 3 h. After cooling to room temperature, the mixture was analysed by ^{1}H and $^{31}P\{^1H\}$ NMR spectroscopy. The spectra showed the presence of alcohol **1**, dabco·BH_3 [δ_H 2.12 and 2.35 (2 × m, 6 H, CH_2); the signal of BH_3 is very broad] and dabco [δ_H 2.44 (s, CH_2)] (N.B. tentative assignment for dabco and dabco·BH_3 is given).

Data for **1**: ^{1}H NMR (C_6D_6): δ 1.51* (td, $^3J_{HH}$ = 6.2, J(H-bond) = 2.4 Hz, 1 H, OH), 3.90 (vt, J' = 1.9 Hz, 2 H), 4.01 (vq, J' = 1.9 Hz, 2 H) and 4.07 (br vt, 4 H) (CH of fc); 4.12* (d, $^3J_{HH}$ = 6.2 Hz, 2 H, CH_2), 7.01–7.09 (m, 6 H) and 7.43–7.51 (m, 4 H) (PPh_2). $^{31}P\{^1H\}$ NMR: δ −16.2 (s). In the reaction mixture, the signals are slightly shifted and those marked with an asterisk collapse into singlets due to a rapid proton exchange.

1′-(Diphenylphosphino)-1-(methoxymethyl)ferrocene–borane (1/1) (10). Alkylation of alcohol **5** was performed similarly to a method found in the literature.[60] Thus, a solution of **7** (830 mg, 2.0 mmol) in dimethylsulphoxide (10 mL) and neat iodomethane (0.85 g, 6 mmol) was introduced *successively* to a stirred suspension of finely ground KOH (225 mg, 4.0 mmol) in dry dimethylsulphoxide (5 mL). The resultant mixture was stirred overnight, diluted with water (50 mL) and extracted with diethyl ether (3 × 15 mL). The organic extracts were washed with water and brine, dried over $MgSO_4$ and evaporated under vacuum. The resulting orange residue was dissolved in a small amount of THF and purified by flash chromatography (silica gel, diethyl ether). A single yellow band was collected and evaporated to afford analytically pure **10** as an orange solid. Yield: 762 mg (89%).

^{1}H NMR ($CDCl_3$): δ *ca.* 0.75–1.80 (very br m, 3 H, BH_3), 3.22 (s, 3 H, CH_2OCH_3), 3.88 (s, 2 H, CH_2OCH_3), 4.07 (vt, J' = 1.9 Hz, 2 H, $C_5H_4CH_2OH$), 4.21 (vt, J' = 1.9 Hz, 2 H, $C_5H_4CH_2OH$), 4.38 (vq, J' = 1.9 Hz, 2 H, $C_5H_4PPh_2$), 4.49 (m, 2 H, $C_5H_4PPh_2$), 7.38–7.50 (m, 8 H, PPh_2), 7.55–7.62 (m, 2 H, PPh_2). $^{13}C\{^1H\}$ NMR ($CDCl_3$): δ 57.79 (CH_2OCH_3), 69.16 (d, $^1J_{PC}$ = 69 Hz, C–P of $C_5H_4PPh_2$), 69.88 (CH_2OCH_3), 70.34, 71.05 (2 × s, 2 C, CH of $C_5H_4CH_2OH$); 72.32 (d, J_{PC} = 8 Hz, 2 C, CH of $C_5H_4PPh_2$), 73.24 (d, J_{PC} = 10 Hz, 2 C, CH of $C_5H_4PPh_2$), 84.77 (s, *C*-CH_2OH of $C_5H_4CH_2OH$), 128.43 (d, J_{PC} = 10 Hz, 4 C, CH of PPh_2), 130.90 (d, J_{PC} = 2 Hz, 2 C, CH of PPh_2), 131.28 (d, $^1J_{PC}$ = 59 Hz, 2 C, C_{ipso} of PPh_2), 132.64 (d, J_{PC} = 10 Hz, 4 C, CH of PPh_2). $^{31}P\{^1H\}$ NMR ($CDCl_3$): δ 16.4 (br d). IR (Nujol): ν/cm^{-1} 2411 s, 2386 vs, 2354 s, 2249 w, 1310 m, 1241 m, 1196 m, 1181 m, 1172 m, 1157 w, 1131 w, 1108 s, 1087 vs, 1058 vs, 1027 s, 952 s, 851 w, 834 m, 818 w, 811 m, 762 m, 746 vs, 705 vs, 640 s, 623 w, 611 m, 592 m, 518 w, 499 vs, 479 m, 467 m, 441 m. EI MS: *m*/*z* (relative abundance) 428 (4, $M^{+\cdot}$), 414 (23, $[M - BH_3]^{+\cdot}$), 399 (12, $[M - Me]^+$), 384 (100, $[M - C_2H_4O]^{+\cdot}$, isobaric with $FcPPh_2{\cdot}BH_3$), 307 (26), 276 (5), 229 (10), 199 (4), 183 (7), 171 (9), 170 (10). HR MS (EI) calc. for $C_{24}H_{26}{}^{11}B^{56}FeOP$ ($M^{+\cdot}$) 428.1164; found 428.1176. Anal. calc. for $C_{24}H_{26}BFeOP$ (428.1): C 67.33, H 6.12%. Found: C 67.25, H 6.14%.

1′-(Diphenylphosphino)-1-(methoxymethyl)ferrocene (11). 1,4-Diazabicyclo[2.2.2]octane (225 mg, 2.0 mmol) and **10** (750 mg, 1.75 mmol) were dissolved in dry toluene (25 mL). The reaction vessel was flushed with argon and sealed with a rubber septum. The mixture was stirred at room temperature overnight and evaporated under vacuum. The residue was taken up with a small amount of THF and transferred to the top of a silica gel column. Elution with hexane–diethyl ether (1 : 1) afforded a single orange band, which was collected and evaporated to give **11** as an orange microcrystalline solid. Yield: 694 mg (96%).

^{1}H NMR ($CDCl_3$): δ 3.24 (s, 3 H, CH_2OCH_3), 3.96 (s, 2 H, CH_2OCH_3), 4.07 (m, 4 H, C_5H_4), 4.16 (vt, J' = 1.8 Hz, 2 H, C_5H_4), 4.34 (vt, J' = 1.8 Hz, 2 H, C_5H_4), 7.28–7.39 (m, 10 H, PPh_2). $^{13}C\{^1H\}$ NMR ($CDCl_3$): δ 57.68 (CH_2OCH_3), 69.77 (s, 2 C, CH of $C_5H_4CH_2OH$), 70.31 (s, CH_2OCH_3), 70.51 (s, 2 C, CH of $C_5H_4CH_2OH$), 71.23 (d, J_{PC} = 4 Hz, 2 C, CH of $C_5H_4PPh_2$), 73.29 (d, J_{PC} = 15 Hz, 2 C, CH of $C_5H_4PPh_2$), 76.25 (d, $^1J_{PC}$ = 6 Hz, C–P of $C_5H_4PPh_2$), 83.75 (s, *C*-CH_2OH of $C_5H_4CH_2OH$), 128.14 (d, J_{PC} = 7 Hz, 4 C, CH of PPh_2), 128.51 (s, 2 C, CH of PPh_2), 130.51 (d, J_{PC} = 20 Hz, 4 C, CH of PPh_2), 139.06 (d, $^1J_{PC}$ = 10 Hz, 2 C, C_{ipso} of PPh_2). $^{31}P\{^1H\}$ NMR ($CDCl_3$): δ −16.3 (s). IR (Nujol): ν/cm^{-1} 1238 m, 1189 s, 1161 s, 1089 vs, 1028 s, 946 s, 829 w, 842 m, 827 m, 749 s, 740 vs, 700 vs, 694 vs, 635 m, 569 m, 529 w, 519 m, 501 vs, 490 s, 462 m, 434 m. EI MS: *m*/*z* (relative abundance) 414 (100, $M^{+\cdot}$), 399 (6, $[M - Me]^+$), 384 (7), 305 (13), 281 (7), 228 (15), 226 (47), 178 (12), 171 (6), 170 (7), 149 (93), 86 (48). HR MS (EI) calc. for $C_{24}H_{23}{}^{56}FeOP$ ($M^{+\cdot}$) 414.0836; found 414.0834. ESI MS: *m*/*z* 415 ($[M + H]^+$), 437 ($[M + Na]^+$), 453 ($[M + K]^+$). Anal. calc. for $C_{24}H_{23}FeOP$ (414.2): C 69.58, H 5.60%. Found: C 69.82, H 5.47%.

Dichlorido(η^6-*p*-cymene)[1′-(diphenylphosphino-κ*P*)-1-(methoxymethyl)ferrocene]ruthenium(II) (12). Di-μ-chloridobis[(η^6-*p*-cymene)chloridoruthenium(II)] (18.5 mg, 0.03 mmol) and **11** (25 mg, 0.06 mmol) were dissolved in dichloromethane (2 mL),

yielding a dark orange-red solution. The solution was stirred for 60 min, filtered through a PTFE syringe filter (0.45 μm) and the filtrate was evaporated under vacuum. The residue was stirred with pentane and diethyl ether (5 mL each) overnight, leaving a solid, which was filtered off and dried under vacuum to afford pure **12**. Yield: 40.5 mg, 94% (red-brown microcrystalline solid).

^{1}H NMR ($CDCl_3$): δ 0.93 (d, $^3J_{HH}$ = 7.0 Hz, 6 H, CH*Me*$_2$), 1.82 (s, 3 H, C_6H_4*Me*), 2.56 (sept, $^3J_{HH}$ = 7.0 Hz, 1 H, C*H*Me$_2$), 3.20 (s, 3 H, CH_2O*Me*), 3.60 and 3.87 (2 × vt, $J' \approx$ 1.9 Hz, 2 H, C_5H_4); 3.96 (s, 2 H, C*H*$_2$OMe), 4.31 (m, 2 H, C_5H_4), 4.49 (vq, $J' \approx$ 1.7 Hz, 2 H, C_5H_4), 5.09 (d, J = 6.2 Hz, 2 H, C_6H_4), 5.16 (dd, J = 6.2, *ca.* 1.3 Hz, 2 H, C_6H_4), 7.39–7.47 (m, 6 H, PPh_2), 7.84–7.91 (m, 4 H, PPh_2). ^{31}P{^{1}H} NMR ($CDCl_3$): δ 19.4 (s). ESI+ MS: *m*/*z* 685 ([M − Cl]$^+$), 649 ([M − Cl − HCl]$^+$). Anal. calc. for $C_{34}H_{37}Cl_2FeOPRu$ (720.4): C 56.68, H 5.18%. Found: C 56.51, H 5.27%.

Reaction of 12 with Ag[SbF$_6$]. Isolation of 13. Di-μ-chlorido-bis[(η^6-*p*-cymene)chloridoruthenium(II)] (15.5 mg, 25 μmol) and **11** (21 mg, 51 μmol) were dissolved in dichloromethane (2 mL) and the solution was stirred for 30 min. To the resulting solution of complex **12** was added Ag[SbF_6] (17 mg, 50 μmol) dissolved in dry MeCN (2 mL) and stirring was continued for another 30 min. The mixture was filtered through a PTFE syringe filter and evaporated. The residue was triturated with diethyl ether and pentane, and dried under vacuum to give essentially pure **13** in practically quantitative yield. An attempted crystallisation from chloroform–hexane afforded several single crystals of **13**·1/2$CHCl_3$ suitable for X-ray diffraction analysis (red irregular block, 0.30 × 0.36 × 0.41 mm^3).

^{1}H NMR ($CDCl_3$): δ 1.16 and 1.19 (2 × d, $^3J_{HH}$ = 6.9 Hz, 3 H, CH*Me*$_2$); 1.88 (s, 3 H, C_6H_4*Me*), 2.13 (d, $^5J_{PH}$ = 1.4 Hz, 3 H, *Me*CN), 2.71 (sept, $^3J_{HH}$ = 6.9 Hz, 1 H, C*H*Me$_2$), 3.29 (s, 3 H, OMe), 3.84 (td, J = 2.5, 1.3 Hz, 1 H), 3.86 (td, J = 2.5, 1.3 Hz, 1 H), 3.90 (m, 1 H), 4.07 (dt, J = 2.5, 1.3 Hz, 1 H), 4.19 (dt, J = 2.5, 1.3 Hz, 1 H), 4.44 (m, 1 H), 4.63 (m, 2 H) and 4.80 (m, 2 H) (8 × CH of C_5H_4); 5.13 and 5.24 (2 × d of unresolved t, J = 6.2 Hz, 1 H, C_6H_4); 5.48 and 5.58 (2 × dd, J = 6.2, 1.5 Hz, 1 H, C_6H_4); 7.51–7.90 (m, 10 H, PPh_2). ^{31}P{^{1}H} NMR ($CDCl_3$): δ 29.7 (s). Anal. calc. for $C_{36}H_{40}ClF_6FeNOPRuSb$·1/2$CHCl_3$ (1021.5): C 42.92, H 4.00, N 1.37%. Found: C 42.66, H 4.32, N 1.24%.

Similar reactions of *in situ* generated **12** with a THF solution of Ag[SbF_6] or, alternatively, with Na[PF_6] in methanol produced only intractable mixtures.

Chlorido(η^2:η^2-cycloocta-1,5-diene)[1′-(diphenylphosphino-κ*P*)-1-(methoxymethyl)ferrocene]rhodium(I) (14). Di-μ-chloridobis [(η^2:η^2-cycloocta-1,5-diene)rhodium(I)] (12.5 mg, 0.025 mmol) and **11** (21 mg, 0.05 mmol) were dissolved in dichloromethane (2 mL). The solution was stirred for 1 h, filtered through a PTFE syringe filter (0.45 μmm) and evaporated under vacuum. The residue was washed with pentane (5 mL) and dried under vacuum to give analytically pure **14** as a yellow-orange amorphous solid. Yield: 33 mg (quant.).

^{1}H NMR ($CDCl_3$): δ 1.87–2.13 and 2.35–2.53 (2 × m, 4 H, CH_2 of cod); 3.13 (m, 2 H, CH═ of cod), 3.34 (s, 3 H, CH_2O*Me*), 4.31 (s, 2 H, C*H*$_2$OMe), 4.38 (d of vt, J = 0.9, 1.9 Hz, 2 H, C_5H_4), 4.40 and 4.45 (2 × vt, $J' \approx$ 1.8 Hz, 2 H, C_5H_4); 4.69 (vq, $J' \approx$ 1.9 Hz, 2 H, C_5H_4), 5.57 (m, 2 H, CH = of cod), 7.32–7.43 (m, 6 H, PPh_2), 7.56–7.73 (m, 4 H, PPh_2). ^{31}P{^{1}H} NMR ($CDCl_3$): δ 23.6 (d, $^1J_{RhP}$ = 151 Hz). ESI+ MS: *m*/*z* 683 ([M + Na]$^+$), 625 ([M − Cl]$^+$; dominant). Anal. calc. for $C_{32}H_{35}ClFeOPRh$ (660.8): C 58.16, H 5.34%. Found: C 57.92, H 5.56%.

Attempted reaction of 11 with [NiCl$_2$(dme)]. A solution of **11** (41.5 mg, 0.10 mmol) in dry dichloromethane (2 mL) was added to a suspension of [$NiCl_2$(dme)] (22 mg, 0.10 mmol; dme = 1,2-dimethoxyethane) suspended in absolute ethanol (2 mL). The mixture was stirred for 1 h and evaporated. Attempted extraction of the evaporation residue led to an extensive decomposition.

***trans*-Dichloridobis[1′-(diphenylphosphino-κ*P*)-1-(methoxymethyl)ferrocene]palladium(II) (*trans*-15).** [$PdCl_2$(cod)] (14.5 mg, 0.05 mmol) and **11** (41.5 mg, 0.10 mmol) were dissolved in dry dichloromethane (2.5 mL) to give a clear red-orange solution. The reaction mixture was stirred for 30 min and filtered through a PTFE syringe filter (0.45 μm pore size). The filtrate was layered with absolute ethanol (5 mL) and the mixture was allowed to crystallise by liquid-phase diffusion for several days. The crystals that formed were filtered off, washed with pentane and dried under vacuum. Yield of *trans*-**15**: 47 mg (93%), red crystals.

^{1}H NMR ($CDCl_3$): δ 3.28 (s, 3 H, CH_2O*Me*), 4.15 (s, 2 H, C*H*$_2$OMe), 4.36 (m, 2 H, C_5H_4), 4.43 (vt, $J' \approx$ 1.8 Hz, 2 H, C_5H_4), 4.53 (m, 2 H, C_5H_4), 4.57 (vt, $J' \approx$ 1.8 Hz, 2 H, C_5H_4), 7.34–7.45 (m, 6 H, PPh_2), 7.60–7.67 (m, 4 H, PPh_2). ^{31}P{^{1}H} NMR ($CDCl_3$): δ 15.4 (s). ESI+ MS: *m*/*z* 1029 ([M + Na]$^+$), 1004 ([M − 2H]$^+$). Anal. calc. for $C_{48}H_{46}Cl_2Fe_2O_2P_2Pd$ (1005.8): C 57.32, H 4.61%. Found: C 57.03, H 4.47%.

Di-μ-chlorido-bis[chlorido{1′-(diphenylphosphino-κ*P*)-1-(methoxymethyl)ferrocene}palladium(II)] (16). [$PdCl_2$(cod)] (28.5 mg, 0.10 mmol) and **11** (41.5 mg, 0.10 mmol) were dissolved in dry dichloromethane (2.5 mL) to give a dark red-brown solution. After stirring for 30 min, the solution was filtered through a PTFE syringe filter (0.45 μm pore size). The filtrate was diluted with absolute ethanol (5 mL) and the mixture was allowed to crystallise at 4 °C overnight. The separated solid was filtered off, washed with pentane and dried under vacuum. Yield of **16**: 41 mg (69%), reddish-brown microcrystalline solid.

^{1}H NMR ($CDCl_3$): δ 3.36 (s, 3 H, CH_2O*Me*), 4.39 (s, 2 H, C*H*$_2$OMe), 4.51 (m, 2 H, C_5H_4), 4.56 (br vq, $J' \approx$ 1.8 Hz, 2 H, C_5H_4), 4.71 (br vt, 2 H, C_5H_4), 4.79 (br s, 2 H, C_5H_4), 7.32–7.65 (m, 10 H, PPh_2). ^{31}P{^{1}H} NMR ($CDCl_3$): δ 31.7 (s). ESI+ MS: *m*/*z* 1207 ([M + Na]$^+$), 555/557 ([Pd(**11**)Cl]$^+$). Anal. calc. for $C_{48}H_{46}Cl_2Fe_2O_2P_2Pd$·$CH_2Cl_2$ (1268.0): C 46.41, H 3.82%. Found: C 46.46, H 3.77% (crystallised from CH_2Cl_2–ethanol).

***In situ* NMR study of the reaction of [Pd(MeCN)$_4$][BF$_4$]$_2$ with 11.** [$Pd(MeCN)_4$][BF_4]$_2$ (4.5 mg, 0.010 mmol) and **11** (8.5 mg, 0.021 mmol) were mixed in dry $CDCl_3$ (*ca*. 0.7 mL; dried over CaH_2). The solid precursors quickly dissolved to afford a deep blue-violet solution. After stirring for 30 min, the reaction mixture was filtered (PTFE syringe filter) and analysed by ^{1}H and ^{31}P NMR spectroscopy. The spectra revealed only very

broad, multiple resonances, which prevented any detailed interpretation.

As a next step, the solution was poured onto solid $[Ph_4As]Cl$ (13.5 mg, *ca.* 0.03 mmol). The arsonium salt dissolved, causing an immediate colour change from the initial deep blue-violet to red-orange and separation of a fine precipitate. After the addition, the mixture was stirred for another 30 min, filtered as above and analysed again by NMR spectroscopy. Comparison of the ^1H and $^{31}P\{^1H\}$ NMR spectra with those of an authentic sample confirmed the presence of *trans*-**15** as the major product (>90%). Two additional complexes (δ_P 15.3 and 15.9) and free **11** (δ_P −16.3) were also detected in the reaction mixture.

Reaction of [PtCl$_2$(cod)] with 11. Ligand **11** (21 mg, 0.05 mmol) and $[PtCl_2(cod)]$ (9.5 mg, 0.025 mmol) were dissolved in dry $CDCl_3$ (1 mL; dried over CaH_2). The solution was stirred for 30 min and analysed by ^1H and ^{31}P NMR spectroscopy. The spectra suggest that *cis*-**17** was formed along with a tiny amount of the corresponding *trans* isomer and liberated cod. The course of the reaction did not change when dichloromethane was used as the solvent and the mixture was evaporated prior to the NMR analysis. Attempts to isolate the isomers in pure form failed.

NMR data for *cis*-17. ^1H NMR ($CDCl_3$): δ 3.23 (s, 3 H, CH_2OMe), 3.81 (vt, J' = 1.9 Hz, 2 H, C_5H_4), 3.97 (s, 2 H, CH_2OMe), 4.02 (vt, J' = 1.9 Hz, 2 H, C_5H_4), 4.17 (br vq, 2 H, C_5H_4), 4.24 (br m, 2 H, C_5H_4), 7.14–7.67 (m, 10 H, PPh_2). $^{31}P\{^1H\}$ NMR ($CDCl_3$): δ 9.8 (s flanked with ^{195}Pt satellites, $^1J_{PtP}$ = 3759 Hz). NMR data for *trans*-**17**. $^{31}P\{^1H\}$ NMR ($CDCl_3$): δ 11.5 (s with ^{195}Pt satellites, $^1J_{PtP}$ = 2622 Hz).

A similar reaction was also performed with equimolar amounts of the starting materials. In this case, ligand **11** (41.5 mg, 0.10 mmol) and $[PtCl_2(cod)]$ (37.5 mg, 0.10 mmol) were reacted in dichloromethane (2 mL) for 30 min and the resulting solution was evaporated under vacuum. NMR analysis of the residue revealed signals attributable to *cis*-**17**, unreacted $[PtCl_2(cod)]$, residual cod and traces of *trans*-**17**.

Aqua-bis[1′-(diphenylphosphino-κ*P*)-1-(methoxymethyl)ferrocene](trifluoromethanesulphonato-κ*O*)copper(I) (10). A solution of ligand **11** (42 mg, 0.10 mmol) in dry $CDCl_3$ (3 mL; distilled from CaH_2) was added to solid $[Cu(CF_3SO_3)]\cdot 1/2PhMe$ (13 mg, 0.050 mmol). The resulting mixture was stirred for 90 min and evaporated under vacuum leaving an oily residue, which was mixed with diethyl ether (*ca.* 8 mL; not dried). The yellow crystalline material which separated after standing at 4 °C overnight was filtered off, washed thoroughly with pentane and dried under vacuum to give **18** as a yellow microcrystalline solid. Yield: 44 mg (83%).

^1H NMR ($CDCl_3$): δ 3.20 (br s, 3 H, CH_2OMe), 3.8 (br s, 2 H, CH_2OMe), 3.98, 4.07, 4.15 and 4.35 (4 × br vt, 2 H, C_5H_4); 7.32–7.48 (br m, 10 H, PPh_2). $^{31}P\{^1H\}$ NMR ($CDCl_3$): δ −7.8 (s). ESI+ MS: *m*/*z* 891 ($[Cu(\mathbf{11})_2]^+$), 535, 477 ($[Cu(\mathbf{11})]^+$), 415 ($[\mathbf{11} + H]^+$). IR (Nujol): ν_{max} 3365 and 3285 br m (ν_{OH}), 1765 composite m, 1587 w, 1571 w, 1304 w, 1290 vs, 1229 vs, 1193 m, 1186 w, 1167 s, 1156 s, 1095 s, 1069 s, 1026 vs, 999 m, 928 m, 837 s, 748 s, 698 s, 632 s, 570 m, 537 m, 513 s, 499 s, 493 s, 466 s, 420 m cm^{-1}. Anal. calc. for $C_{49}H_{48}CuF_3Fe_2O_6P_2S$ (1059.1): C 55.56, H 4.57%. Found: C 55.72, H 4.52%.

X-Ray crystallography

Single crystals suitable for X-ray diffraction analysis were grown as described in ESI.† The full-set diffraction data ($\pm h \pm k \pm l$; θ_{max} = 26.0–27.5°, data completeness ≥99%) were collected with Nonius Kappa CCD or Bruker Apex II CCD diffractometers equipped with a Cryostream Cooler (Oxford Cryosystems) at 150(2) K using graphite monochromated MoKα radiation (λ = 0.71073 Å). If appropriate, the data were corrected for absorption by methods incorporated in the diffractometer software.

The structures were solved by the direct methods (SIR97[61]) and refined by full-matrix least squares on F^2 (SHELXL97[62]). Unless noted otherwise, the non-hydrogen atoms were refined with anisotropic displacement parameters. The OH and BH hydrogens were identified on difference density maps and were refined as riding atoms with U_{iso} assigned to $1.2U_{eq}$ of their bonding atoms (O and B). Other hydrogen atoms were included at their calculated positions and refined as riding atoms. Relevant crystallographic data and structure refinement parameters are available as ESI (Tables S1 and S2†). Particular details on structure refinement are as follows.

Two of four CH_2OH independent moieties in the structure of **5** are disordered and their C and O atoms were refined with isotropic displacement parameters. The selected crystal of **10** suffered from non-merohedral twinning. The data were corrected by PLATON[63] and the contribution of the minor component was refined to *ca.* 7.4%.

The refinement of the structure model for complex **16**·CH_2Cl_2 was complicated by disorder. First, one of the cyclopentadienyl rings bearing the CH_2OMe pendant was rotationally disordered and was modelled over two equally populated positions. Second, the solvent molecules were clearly detected in structural voids but could not be refined. A new data set was therefore generated using the SQUEEZE[64] algorithm as incorporated in the PLATON program. A total of 172 electrons were found in the 476 Å^3 void space per unit cell (*N.B.* four molecules of dichloromethane represent 168 electrons).

All geometric data and structural drawings were obtained with a recent version of the PLATON program. The numerical values are rounded with respect to their estimated deviations (ESDs) given to one decimal place. Parameters relating to atoms in constrained positions are given without ESDs.

Acknowledgements

This work was supported by the Czech Science Foundation (project no. P207/10/0176) and is a part of a long-term research plan supported by the Ministry of Education, Youth and Sports of the Czech Republic (project no. MSM0021620857).

Notes and references

1 G. P. Sollott, H. E. Mertwoy, S. Portnoy and J. L. Snead, *J. Org. Chem.*, 1963, **28**, 1090.

2 G. P. Sollott, J. L. Snead, S. Portnoy, W. R. Peterson and H. E. Mertwoy, *U.S. Dept. Com., Office Tech. Serv., PB Report*, 1965, vol. **II**, 441 [*Chem. Abstr.*, 1965, **63**, 18174].

3 *Ferrocenes: Ligands, Materials and Biomolecules*, ed. P. Štěpnička, Wiley, Chichester, 2008.

4 Selected reviews: (*a*) R. C. J. Atkinson, V. Gibson and N. J. Long, *Chem. Soc. Rev.*, 2004, **33**, 313; (*b*) P. Barbaro, C. Bianchini, G. Giambastiani and S. L. Parisel, *Coord. Chem. Rev.*, 2004, **248**, 2131; (*c*) R. Goméz Arrayás, J. Adrio and J. C. Carretero, *Angew. Chem., Int. Ed.*, 2006, **45**, 7674.

5 P. Štěpnička, 1′-Functionalised ferrocene phosphines: synthesis, coordination chemistry and catalytic applications, in *Ferrocenes: Ligands, Materials and Biomolecules*, ed. P. Štěpnička, Wiley, Chichester, 2008, ch. 5, pp. 177–204.

6 For recent examples, see: Y = OH: (*a*) R. C. J. Atkinson, V. C. Gibson, N. J. Long and A. J. P. White, *Dalton Trans.*, 2010, **39**, 7540; Y = $B(2,4,6\text{-}Me_3C_6H_2)_2$: (*b*) M. W. P. Bebbington, S. Bontemps, G. Bouhadir, M. J. Hanton, R. P. Tooze, H. van Rensburg and D. Bourissou, *New J. Chem.*, 2010, **34**, 1556; Y = CH_2(benzimidazolium): (*c*) S. Gülcemal, A. Labande, J.-C. Daran, B. Çetinkaya and R. Poli, *Eur. J. Inorg. Chem.*, 2009, 1806; Y = Fc: (*d*) M. Lohan, B. Milde, S. Heider, J. M. Speck, S. Krausse, D. Schaarschmidt, T. Rüffer and H. Lang, *Organometallics*, 2012, **31**, 2310; Y = 2-Py, 3-Py and CH_2(2-Py) (Py = pyridyl): (*e*) P. Štěpnička, J. Schulz, T. Klemann, U. Siemeling and I. Císařová, *Organometallics*, 2010, **29**, 3187; (*f*) U. Siemeling, T. Klemann, C. Bruhn, J. Schulz and P. Štěpnička, *Dalton Trans.*, 2011, **40**, 4722; (*g*) U. Siemeling, T. Klemann, C. Bruhn, J. Schulz and P. Štěpnička, *Z. Anorg. Allg. Chem.*, 2011, **637**, 1824; Y = CH_2NMe_2: (*h*) P. Štěpnička, M. Zábranský and I. Císařová, *ChemistryOpen*, 2012, **1**, 71; Y = CH_2PPh_2: (*i*) P. Štěpnička, I. Císařová and J. Schulz, *Organometallics*, 2011, **30**, 4393; (*j*) P. Štěpnička and I. Císařová, *J. Organomet. Chem.*, 2012, **716**, 110; Y = CO_2SnR_3: (*k*) P. Štěpnička, I. Císařová and A. Růžička, *J. Organomet. Chem.*, 2010, **695**, 271; Y = CONHR (R = H, Cy, Ph, NH_2): (*l*) P. Štěpnička, H. Solařová, M. Lamač and I. Císařová, *J. Organomet. Chem.*, 2010, **695**, 2423; (*m*) P. Štěpnička, H. Solařová and I. Císařová, *J. Organomet. Chem.*, 2011, **696**, 3727; Y = $CONHCH_2(2\text{-}C_6H_4PPh_2)$: (*n*) P. Štěpnička, M. Krupa, M. Lamač and I. Císařová, *J. Organomet. Chem.*, 2009, **694**, 2987; Y = CONHCH(R)-CO_2Me and related compounds: (*o*) J. Tauchman, I. Císařová and P. Štepnička, *Organometallics*, 2009, **28**, 3288; (*p*) J. Tauchman, I. Císařová and P. Štěpnička, *Eur. J. Org. Chem.*, 2010, 4276; (*q*) J. Tauchman, I. Císařová and P. Štěpnička, *Dalton Trans.*, 2011, **40**, 11748; (*r*) J. Tauchman, B. Therrien, G. Süss-Fink and P. Štěpnička, *Organometallics*, 2012, **31**, 3985; Y = $CONH_{(2-n)}(CH_2CH_2OH)_n$ (n = 1, 2): (*s*) J. Schulz, I. Císařová and P. Štěpnička, *J. Organomet. Chem.*, 2009, **694**, 2519; Y = $CONH(CH_2)_nSO_3[HNEt_3]$ (n = 1–3): (*t*) J. Schulz, I. Císařová and P. Štěpnička, *Organometallics*, 2012, **31**, 729.

7 P. Štěpnička and T. Baše, *Inorg. Chem. Commun.*, 2001, **4**, 682.

8 (*a*) M. D. Wright, *Organometallics*, 1990, **9**, 853; (*b*) I. R. Butler and R. L. Davies, *Synthesis*, 1996, 1350.

9 J. Podlaha, P. Štěpnička, J. Ludvík and I. Císařová, *Organometallics*, 1996, **15**, 543.

10 P. Štěpnička, *Eur. J. Inorg. Chem.*, 2005, 3787.

11 The planar-chiral isomer, (S_p)-[Fe(η^5-C_5H_3-1-CH_2OH-2-PPh_2)(η^5-C_5H_5)], has been prepared from (*a*) (S_p)-2-(diphenylphosphino)-1-{(*S*)-[(2-methoxymethyl)pyrrolidin-1-yl]-methyl}ferrocene: C. Ganter and T. Wagner, *Chem. Ber.*, 1995, **128**, 1157; and from (*b*) (S_p)-**4**: O. Riant, O. Samuel, T. Flessner, S. Taudien and H. B. Kagan, *J. Org. Chem.*, 1997, **62**, 6733.

12 (*a*) G. Argouarch, O. Samuel and H. B. Kagan, *Eur. J. Org. Chem.*, 2000, 2885; (*b*) I. R. Butler, P. K. Baker, G. R. Eastham, K. M. Fortune, P. N. Horton and M. B. Hursthouse, *Inorg. Chem. Commun.*, 2004, **7**, 1049; (*c*) J. Cabou, J. Brocard and L. Pélinski, *Tetrahedron Lett.*, 2005, **46**, 1185; (*d*) R. Šebesta, F. Bilčík and B. Horváth, *Eur. J. Org. Chem.*, 2008, 5157.

13 Phosphine substituents have been typically protected as the corresponding P-sulphides: (*a*) L. Routaboul, S. Vincendeau, J.-C. Daran and E. Manoury, *Tetrahedron: Asymmetry*, 2005, **16**, 2685; (*b*) L. Routaboul, S. Vincendeau, C.-O. Turrin, A.-M. Caminade, J.-P. Majoral, J.-C. Daran and E. Manoury, *J. Organomet. Chem.*, 2007, **692**, 1064; (*c*) A. Labande, J.-C. Daran, E. Manoury and R. Poli, *Eur. J. Inorg. Chem.*, 2007, 1205; (*d*) C. Audin, J.-C. Daran, E. Deydier, E. Manoury and R. Poli, *C. R. Chim.*, 2010, **13**, 890.

14 E. R. Burkhardt and K. Matos, *Chem. Rev.*, 2006, **106**, 2617 and references therein.

15 (*a*) J. M. Brunel, B. Faure and M. Maffei, *Coord. Chem. Rev.*, 1998, **178–180**, 665; (*b*) M. Ohff, J. Holz, M. Quirmbach and A. Boerner, *Synthesis*, 1998, 1391.

16 (*a*) A. Bader and E. Lindner, *Coord. Chem. Rev.*, 1991, **108**, 27; (*b*) C. S. Slone, D. A. Weinberger and C. A. Mirkin, *Prog. Inorg. Chem.*, 1999, **48**, 243; (*c*) P. Braunstein and F. Naud, *Angew. Chem., Int. Ed.*, 2001, **40**, 680.

17 D.-H. Kim, E.-S. Ryu, C. S. Cho, S. C. Shim, H.-S. Kim and T.-J. Kim, *Organometallics*, 2000, **19**, 5748.

18 L. Routaboul, J. Chiffre, G. G. A. Balavoine, J.-C. Daran and E. Manoury, *J. Organomet. Chem.*, 2001, **637–639**, 364.

19 S. Bhattacharyya, *J. Chem. Soc., Perkin Trans. 1*, 1996, 1381.

20 S. Bhattacharyya, *J. Chem. Soc., Dalton Trans.*, 1996, 4617.

21 S. Bhattacharyya, *Synlett*, 1996, 971.

22 S. Bhattacharyya, *Organometallics*, 1996, **15**, 1065.

23 The compound was identified by its NMR spectra. ^{1}H NMR ($CDCl_3$): δ *ca.* 0.80–1.70 (very br m, 3 H, BH_3), 4.09 (s, 5 H, C_5H_5), 4.42 (vq, $J' \approx 2$ Hz, 2 H, $C_5H_4PPh_2$), 4.51 (m, 2 H, $C_5H_4PPh_2$), 7.37–7.62 (m, 10 H, PPh_2). $^{31}P\{^1H\}$ NMR ($CDCl_3$): δ *ca.* 16.6 (broad signal).

24 $FcPPh_2$ results from accidental protonolysis of 1′-(diphenylphosphino)-1-lithioferrocene, which is generated *in situ* and treated with *N*,*N*-dimethylformamide to afford **2**. The phosphine typically remains present (albeit in tiny amounts) even after flash chromatography and crystallisation of the aldehyde. For examples of the synthetic use of 1′-(diphenylphosphino)-1-lithioferrocene, see ref. 5 and 8*b*.
25 See, for instance: http://www.organic-chemistry.org/chemicals/reductions/boranes.shtm (retrieved on September 10, 2012).
26 H. Anane, A. Boutalib and F. Tomás, *J. Phys. Chem. A*, 1997, **101**, 7879.
27 I. R. Butler and R. L. Davies, *Synthesis*, 1996, 1350 and references cited therein.
28 G. Gasser, A. J. Fischmann, C. M. Forsyth and L. Spiccia, *J. Organomet. Chem.*, 2007, **692**, 3835.
29 P. Štěpnička and I. Císařová, *New J. Chem.*, 2002, **26**, 1389.
30 (*a*) K. J. Donaghy, P. J. Caroll and L. G. Sneddon, *Inorg. Chem.*, 1997, **36**, 57; (*b*) N. Oohara, K. Katagiri and T. Imamoto, *Tetrahedron: Asymmetry*, 2003, **17**, 2171; (*c*) Y. Wang, W. Weissensteiner, K. Mereiter and F. Spindler, *Helv. Chim. Acta*, 2006, **89**, 1772.
31 A. M. Makal, D. Plazuk, J. Zakrzewski, B. Misterkiewicz and K. Wozniak, *Inorg. Chem.*, 2010, **49**, 4046.
32 D. W. Slocum and C. R. Ernst, *Adv. Organomet. Chem.*, 1972, **10**, 79.
33 (*a*) M. P. Brown and R. W. Heseltine, *J. Chem. Soc., Chem. Commun.*, 1968, 1551; (*b*) M. P. Brown, R. W. Heseltine, P. A. Smith and P. J. Walker, *J. Chem. Soc. A*, 1970, 410; (*c*) R. H. Crabtree, P. E. M. Siegbahn, O. Eisenstein, A. L. Rheingold and T. F. Koetzle, *Acc. Chem. Res.*, 1996, **29**, 348; (*d*) R. Custelcean and J. E. Jackson, *Chem. Rev.*, 2001, **101**, 1963.
34 A search in CSD (version 5.33 from November 2011 with updates up to August 2012) for intermolecular $BH_3\cdots OH$ contacts with H···H distance 1.0–2.5 Å and H-bond angle >120° resulted in 23 hits: (refcodes) ABUKAJ, ADIMOP, ADINAC, ADINEG, AGEYUH, AVOCAQ, CENJIP, DAZPIE, DUZNUI, GOCVEZ, GOCVID, GOKHET, IBATUC, IQEXUY, IQEYAF, LICTIA, OLEVEH, REFCUB, SIQZEY, VADNIZ, WAGBAH, XAFNAT, WANTAI.
35 These compounds have been prepared and studied intentionally; see ref. 33*d*.
36 Significant intermolecular BH···H–O contacts were detected in ten of 23 structurally characterised borane adducts of (amino)phosphino-alcohols and phenols (refcodes AVOCAQ, IBATUC, IQEXUY, IQEAF, LICTIA, OLEVEH, REFCUB, SIQZEY, VADNIZ, WAGBAH) for which the *coordinates* are available (H···H distances = 1.57–2.44 Å, H···H–O angles = *ca.* 125–170°).
37 The flexibility of the crystal assembly of **8** is further manifested by the crystal structure at room temperature, which is totally disordered, not allowing even for a reliable determination of the lattice parameters, but becomes gradually ordered during cooling.
38 (*a*) E. A. Cookson and P. C. Crofts, *J. Chem. Soc. C*, 1966, 2003; (*b*) T. B. Rauchfuss, F. T. Pation and D. M. Roundhill, *Inorg. Chem.*, 1975, **14**, 652; (*c*) W. E. McEwen, J. E. Fountaine, D. N. Schulz and W.-I. Shia, *J. Org. Chem.*, 1976, **41**, 1684; (*d*) C. Andersson, J. Friedrich, M. H. Johansson and Å. Oskarsson, *J. Mol. Struct.*, 1999, **479**, 1; (*e*) S. Sjövall, M. Johansson and C. Andersson, *Organometallics*, 1999, **18**, 2198.
39 Selected examples: (*a*) W. E. McEwen, A. B. Janes, J. W. Knapczyk, V. L. Kyllingstad, W.-I. Shiau, S. Shore and J. H. Smith, *J. Am. Chem. Soc.*, 1978, **100**, 7304; (*b*) G. K. Anderson and R. Kumar, *Inorg. Chem.*, 1984, **23**, 4064; (*c*) E. Lindner, S. Meyer, P. Wegner, B. Karle, A. Sickinger and B. Steger, *J. Organomet. Chem.*, 1987, **335**, 59; (*d*) E. Lindner, R. Speidel, R. Fawzi and W. Hiller, *Chem. Ber.*, 1990, **123**, 2255; (*e*) B. de Klerk-Engels, J. H. Groen, K. Vrieze, A. Möckel, E. Lindner and K. Goubitz, *Inorg. Chim. Acta*, 1992, **195**, 237; (*f*) E. Lindner, A. Möckel, H. A. Mayer, H. Kühbauch, R. Fawzi and R. Steiman, *Inorg. Chem.*, 1993, **32**, 1266; (*g*) E. Lindner, Q. Wang, H. A. Mayer and A. Bader, *J. Organomet. Chem.*, 1993, **458**, 229; (*h*) E. Lindner, M. Haustein, H. A. Mayer, H. Kühbauch, K. Vrieze and B. de Klerk-Engels, *Inorg. Chim. Acta*, 1994, **215**, 165; (*i*) W. A. Herrmann, C. Brossmera, K. Öfele, M. Beller and H. Fischer, *J. Mol. Catal. A: Chem.*, 1995, **103**, 133; (*j*) E. Lindner, S. Pautz, R. Fawzi and M. Steimann, *Organometallics*, 1998, **17**, 3006; (*k*) C. W. Rogers, B. O. Patrick, S. J. Rettig and M. O. Wolf, *J. Chem. Soc., Dalton Trans.*, 2001, 1278.
40 R. C. J. Atkinson, V. C. Gibson, N. J. Long, A. J. P. White and D. J. Williams, *Organometallics*, 2004, **23**, 2744.
41 The related planar-chiral ligand, $[Fe\{\eta^5\text{-}C_5H_3(PPh_2\text{-}1)(OMe\text{-}2)\}_2]$, has been reported by Zhang *et al.*: F. Xie, D. Liu and W. Zhang, *Tetrahedron Lett.*, 2008, **49**, 1012.
42 K. D. Redwine, H. D. Hansen, S. Bowley, J. Isbell, D. Vodak and J. H. Nelson, *Synth. React. Inorg. Met.-Org. Chem.*, 2000, **30**, 409.
43 P. Štěpnička, J. Demel and J. Čejka, *J. Mol. Catal. A: Chem.*, 2004, **224**, 161.
44 For a recent example of the use of these two complementary synthetic approaches, see: M. V. Jiménez, J. J. Pérez-Torrente, M. I. Bartolomé, E. Vispe, F. J. Lahoz and L. A. Oro, *Macromolecules*, 2009, **42**, 8146.
45 The reaction of $[Pd(MeCN)_4](CF_3SO_3)_2$ with 2-$Ph_2PC_6H_4CH_2OMe$ (**L**) was shown to produce the stable bischelate complex *cis*-$[Pd(\mathbf{L}\text{-}\kappa^2O,P)](TfO)_2$: C. Andersson, J. Friedrich, M. H. Johansson and Å. Oskarsson, *J. Mol. Struct.*, 1999, **479**, 1.
46 The $^{31}P\{^1H\}$ NMR spectrum of the reaction mixture contains several broad signals (δ_P *ca.* 26.0, 32.5 and 33.3).
47 The presence of two additional minor Pd-**11** species (δ_P 15.3 and 15.9) and free **11** in the crude reaction mixture may well reflect a departure from the ideal stoichiometry at the small reaction scale.

48 The crystal structure of *cis*-**17** was determined but could not be satisfactorily refined due to a poor quality of the data (crystal) available. Nevertheless, the connectivity established by X-ray analysis is unequivocal and confirms the *cis* geometry of the complex.

49 Free **11** (2 mg) was added to a pre-formed solution of *cis*-**17** (0.025 mmol in *ca.* 0.7 mL $CDCl_3$) and the composition of the mixture was regularly monitored by the ^1H and ^{31}P NMR spectra. After the addition, the amount of *trans*-**17** gradually increased from the initial *ca.* 3 mol% to 20 mol% after 14 days. The isomerisation then stopped. A similar *cis–trans* ratio of *ca.* 80 : 20 was determined for the product resulting from the reaction between $[PtCl_2(cod)]$ and an excess of **11** (Pt–P ≈ 1 : 2.1) in dichloromethane.

50 P. Štěpnička, J. Podlaha, R. Gyepes and M. Polášek, *J. Organomet. Chem.*, 1998, **552**, 293.

51 Selected achiral compounds. (*a*) Y = $P(O)Ph_2$: R. J. Coyle, Y. L. Slovokhotov, M. Y. Antipin and V. V. Grushin, *Polyhedron*, 1998, **17**, 3059; (*b*) Y = SMe: V. C. Gibson, N. J. Long, A. J. P. White, C. K. Williams, D. J. Williams, M. Fontani and P. Zanello, *J. Chem. Soc., Dalton Trans.*, 2002, 3280; (*c*) Y = PO_3Et_2: P. Štěpnička, I. Císařová and R. Gyepes, *Eur. J. Inorg. Chem.*, 2006, 926; (*d*) Y = Py and CH_2Py (Py = 2-pyridyl): ref. 6*e*; (*e*) Y = $CH{=}CH_2$: P. Štěpnička and I. Císařová, *Collect. Czech. Chem. Commun.*, 2006, **71**, 215; (*f*) Y = $CONH_2$ and $CONHNH_2$: ref. 6*m*; (*g*) Y = CONHPh: ref. 6*l*; (*h*) Y = $CONHCH_2CH_2OH$ and $CON(CH_2CH_2OH)_2$: ref. 6*s*; (*i*) Y = $CONHCH_2CH_2Py$: J. Kühnert, M. Dušek, J. Demel, H. Lang and P. Štěpnička, *Dalton Trans.*, 2007, 2802; (*j*) Y = $CONHCH_2CONH_2$: ref. 6*o*; (*k*) Y = $COCH_2NHSO_3(HNEt_3)$: ref. 6*t*.

52 For a representative example from the chemistry of ferrocene ligands, see: G. Pilloni, B. Corain, M. Degano, B. Longato and G. Zanotti, *J. Chem. Soc., Dalton Trans.*, 1993, 1777.

53 G. A. Lawrance, *Chem. Rev.*, 1986, **86**, 17.

54 According to a search in the Cambridge Structural Database, version 5.33 of November 2011 with updates in November 2011, and in February, May and August 2012.

55 D. A. Knight and S. W. Keller, *J. Chem. Crystallogr.*, 2006, **36**, 531.

56 $[L_2Cu_2(H_2O)_2]X_2$, where L = bis[5-*tert*-butyl-2-(diphenylphosphino)-methyl-1-methoxyphenyl]methane, and X = ClO_4 and BF_4: X.-T. Meng, Q.-S. Li, F.-B. Xu, H.-B. Song, C. E. Anson and Z.-Z. Zhang, *Inorg. Chem.*, 2006, **45**, 7986.

57 T.-Y. Dong and L.-L. Lai, *J. Organomet. Chem.*, 1996, **509**, 131.

58 R. A. Zelonka and M. C. Baird, *Can. J. Chem.*, 1972, **50**, 3063.

59 D. Drew and J. R. Doyle, *Inorg. Synth.*, 1972, **13**, 47.

60 H. Plenio, J. Hermann and A. Sehring, *Chem.–Eur. J.*, 2000, **6**, 1820.

61 A. Altomare, M. C. Burla, M. Camalli, G. L. Cascarano, C. Giacovazzo, A. Guagliardi, A. G. G. Moliterni, G. Polidori and R. Spagna, *J. Appl. Crystallogr.*, 1999, **32**, 115.

62 G. M. Sheldrick, *Acta Crystallogr., Sect. A: Fundam. Crystallogr.*, 2008, **64**, 112.

63 A. L. Spek, *J. Appl. Crystallogr.*, 2003, **36**, 7.

64 P. van der Sluis and A. L. Spek, *Acta Crystallogr., Sect. A: Fundam. Crystallogr.*, 1990, **46**, 194.